A CENTURY OF TRANSITIONS IN NEW YORK CITY'S MEASLES DYNAMICS

A CENTURY OF TRANSITIONS IN NEW YORK CITY'S MEASLES DYNAMICS

By

KARSTEN HEMPEL, B.Sc.

A Thesis

Submitted to the school of Graduate Studies

in Partial Fulfillment of the Requirements

for the Degree

of Master of Science

McMaster University

MASTER OF SCIENCE (2012) McMaster University
(Mathematics) Hamilton, Ontario

TITLE:	A CENTURY OF TRANSITIONS IN NEW YORK CITY'S MEASLES DYNAMICS
AUTHOR:	Karsten Hempel, B.Sc. (MTA)
SUPERVISOR:	Dr. David Earn
NUMBER OF PAGES:	viii, 46

Abstract

Infectious diseases spreading in a human population can occasionally exhibit sudden transitions in their qualitative dynamics. Previous work has been very successful in predicting such transitions in New York City's measles incidence rates using the standard SIR model (*susceptible, infected, recovered*). This work relied on a dataset spanning 45 years, which we have extended to 93 years (1891-1984). We continue previous research in transition analysis on this larger dataset, and compare resonant and transient periods predicted to exist in NYC's measles incidence rates with those observed through a continuous wavelet transform of the data. We find good agreement between SIR predictions and observation, and in particular note the likely existence of previously unobserved hysteresis early in our new time-series.

Acknowledgments

I would like to acknowledge my supervisor Dr. David Earn, for all his contributions, advice and feedback during the preparation of the present work. I owe much personal and professional growth to his invaluable guidance. I would also like to acknowledge Arlene Shaner (Reference Librarian and Acting Curator, Rare Books & Manuscripts) and the New York Academy of Medicine Library for their indispensable cooperation in compiling the dataset used in this paper.

Contents

List of Figures

1 Introduction

A mechanistic mathematical model is a scientific tool that represents the governing causal mechanics of a system of natural phenomena in mathematical terms. The application of mathematical modeling to biological systems, and in particular to the spread of infectious diseases within human populations, has proven to be a very powerful method for understanding and predicting natural dynamics [4, 10, 11, 14]. One general approach to this type of study is to acquire historical records of aggregated cases of infection for a particular population, and to attempt to use a mechanistic mathematical model to make sense of the data, and this is indeed our an approach for the case of measles in New York City (NYC).

1.1 Measles in the 20th century

A case study on a population and disease requires precision at various levels. First, when considering the types of public health records within which cases of infection are usually reported, one must have reason to believe that the disease in question has been accurately reported throughout the population. Measles is a childhood viral infection to which the human body usually, following recovery, develops permanent immunity. Measles was endemic to most populations in the world prior to the development and thorough distribution of its vaccine, which was first introduced to the NYC population in 1963. Its high prevalence (nearly everyone became infected at some point in their lives), combined with a very recognizable symptom (koplik's spots), resulted in very accurate reporting of cases which were brought to the attention of a medical professional. Furthermore, its symptoms are such that infected individuals (usually children) were very likely to be seen by a medical professional who was required by law to report cases to a central body, which resulted in health institutions acquiring accurate counts of measles cases. As vaccine uptake increased after 1963, the total number of measles cases per unit of time dropped drastically, and eventually the disease was virtually removed from the NYC population, with at most small outbreaks occurring periodically. With medical professionals encountering the disease less often, and the general population becoming less aware of its symptoms, the quality of measles reporting decreased following vaccination. In this paper, we present a case study of measles in NYC while the total number of cases was high, relying on the accuracy of reporting as a result.

1.2 The dataset

In 1973, London and Yorke [20] published measles incidence rates for NYC spanning the years of 1928–1973. The published data are aggregated monthly totals of measles cases for the whole of NYC for the duration of the noted time span. This dataset has been extensively studied [6, 8, 10, 20, 22], and this fact in part motivated the undertaking of the research presented in this paper. We extend the dataset to span a wider range of dates, and in addition improve the quality of at least part of the data published by London and Yorke [20]. Compiling data from various sources, we produce a time-series that includes aggregated counts of reported measles cases for all of NYC, along with concurrent demographic data (total population and total births), which spans the 94 years 1891–1984, more than doubling the length of the time series. §2 details the process of data acquisition, compilation, and quality-checking that was undertaken.

1.3 Compartmental Modeling of Infectious Diseases

Mathematical epidemiological modeling is often done by compartmentalizing the population according to possible states related to infection, and by representing the rates of transfer between these states as a system of ordinary differential equations (ODEs). The SIR model is a very common compartmental model used for diseases that confer permanent immunity to recovered individuals, as is the case for measles [4, 10, 17]. The acronym "SIR" stands for the compartments of the model, which are *Susceptible*, *Infected*, and *Recovered*. This model is the simplest possible compartmental model describing this type of disease, and numerous modifications and extensions of the model have been developed to improve on inadequacies of this simple form. However, Krylova and Earn [18,19] showed that for measles, the simple version of the SIR model is sufficient for our purposes (details in §3.1).

1.4 Spectral Analysis

Measles, like many other infectious diseases, exhibits recurrent epidemics within a population, and the pattern of recurrence in part resonates with the seasonal year. This occurs for numerous reasons, but for measles the primary reason is the systematic change in population behaviour from winter to summer, and in particular the gathering of children in schools during the winter [20]. Yearly outbreaks of measles, however, are not fixed in size. For instance, measles is often observed to exhibit a biennial pattern of alternation between a small epidemic one year and a large epidemic the next. Moreover, measles dynamics are not limited to annual and

biennial patterns, and in fact analyzing the frequency structure of a measles time-series can be very informative when trying to understand the governing mechanics of its epidemiology. This is true because the frequency structures of disease time-series can shift suddenly due to small changes in demographic conditions [11]. In the measles data we will be examining, for instance, a sudden transition from an annual cycle to a biennial cycle, and the reverse, can be observed (see Figure 13 for a plot of the complete time series). Understanding these transitions using the SIR model — the central goal of this paper — is done by using a parameterized version of the model [19] along with demographic data to determine predicted behaviour of the time series, and comparing these predictions with the actual patterns observed in the data. Previous research [10, 19] has shown good agreement between predictions of the SIR model with patterns observed in the NYC measles data published by London and Yorke [20], and we extend this analysis for our new extended dataset.

2 The Data

We compiled data from a number of sources, some of which have — to our knowledge — not yet been made available in digital form. As a result, it is important to understand these sources, and to verify the accuracy of the data as we proceed in compiling them into a larger set. Moreover, the time-series we will construct is a patchwork, and may inherit sudden shifts in systematic inaccuracies from its disparate sources, a possibility against which we must control. We will attempt to deal with any such problems in the coming section. For summaries of which data are available and which are used for compilation into a continuous time-series, refer to §2.8, Tables 1 and 2.

2.1 Required Data

For our analyses, we make use of the following types of data tables:

- Weekly and monthly tabulated total reported cases of measles for all of NYC.
- Yearly tabulated total reported births for all of NYC.
- Yearly tabulated total population for all of NYC.

2.2 Data Sources

The compiled disease data sets span 1891–1984, and were pieced together from four different sources:

1. 1891–1932: Newly digitized weekly data from weekly bulletins published by the NYC Health Dept. (§2.3).
2. 1928–1973: Monthly data published by London and Yorke [20].
3. 1958–1976: Newly digitized weekly data recorded by the NYC Health Dept. (§2.4).
4. 1976–1984: Monthly data available online in the NYC Heath Dept. Annual Vital Statistics Reports [1].

Demographic data, namely total reported births and total population data were pieced together from two sources:

1. 1891–1932: Newly digitized weekly data from weekly bulletins published by the NYC Health Dept.. (§2.3.2), which included vital data.
2. 1900–1950: 5-year totals from the NYC Heath Dept. Vital Statistics Reports [1]
3. 1950–1984: Yearly totals from the NYC Heath Dept. Vital Statistics Reports [1]

§3.1 describes the use of birth information in the SIR model, and it is important to note that what is actually of interest is the number of new individuals entering the population that are susceptible to measles. When children are vaccinated against measles, this number is reduced, and so vaccination data is required in order to properly conduct our analysis. However, we do not extend our analysis far past the introduction of the measles vaccine in 1963 for reasons noted in §1.1. We use the same vaccination rates as Krylova and Earn [19] for 1963–1973, and assume that the proportion of newborns vaccinated in NYC remains high ($\approx$95%) until 1984.

2.3 The Health Dept. Bulletins: 1891–1932 Weekly Data

Near the end of the 19th century and in the first half of the 20th, the NYC Health Department published weekly bulletins containing information regarding a wide variety of public health related issues (see Appendix B for sample photographs of such a bulletin). Some of the details provided in these bulletins were incidence rates for numerous infectious diseases, including measles. Spanning the years 1891–1932, the weekly bulletins were published in two volumes. We acquired access to these through

the NYC Academy of Medicine Library [1] As noted previously, vital statistics for the whole of NYC were acquired through the NYC Health Dept., which provides data going back to 1900 [1]. However, we require data going back to the beginning of measles incidence data in 1891. To fill in the missing years of 1891–1899, we extracted vital statistics from the health bulletins.

An important note must be made about these bulletins regarding their reporting area. The data tables in the bulletins provide data for only Manhattan Island up until 15 January 1898, after which the reporting area was enlarged to cover Manhattan, The Bronx, Brooklyn, Queens, and Richmond. We wish to retain as high consistency as possible between the reporting area of both measles incidence data and vital statistics. It is therefore advantageous to use disease incidence data and vital statistics from the same source, especially through a change in reporting area.

2.3.1 Disease Incidence, Volume 1: 1891–1914

City-wide reported cases of measles were extracted from a table as shown in Figure 1.

[1]The NYC Academy of Medicine [2] is a public institution independent of the NYC Health Department. Its library maintains a collection of books and literature related to health in the NYC population throughout its history.

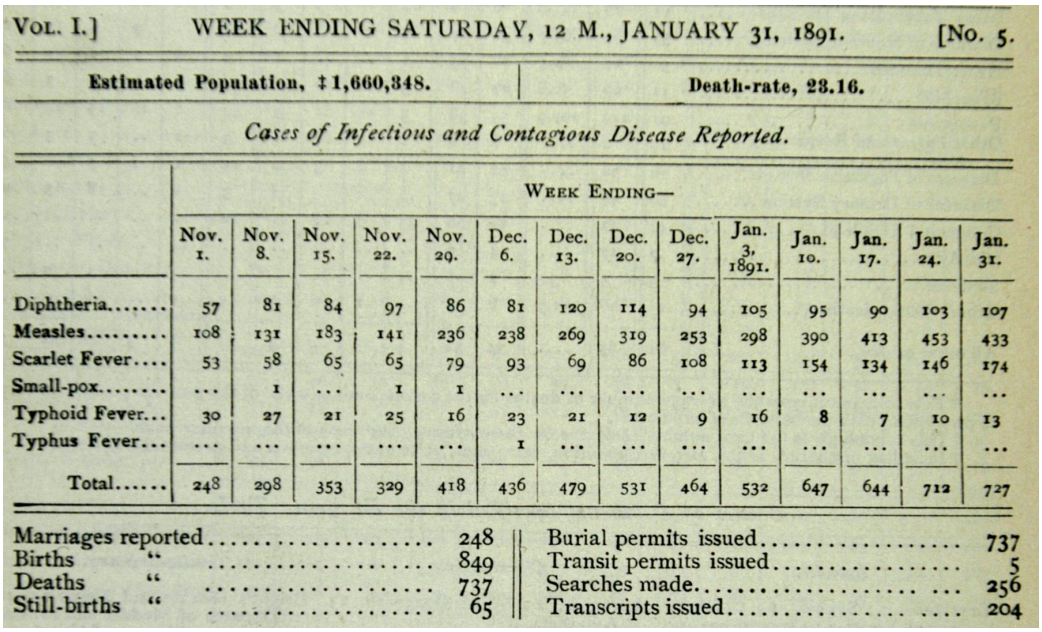

VOL. I.] WEEK ENDING SATURDAY, 12 M., JANUARY 31, 1891. [NO. 5.

Estimated Population, ‡1,660,348. | **Death-rate, 23.16.**

Cases of Infectious and Contagious Disease Reported.

	WEEK ENDING—													
	Nov. 1.	Nov. 8.	Nov. 15.	Nov. 22.	Nov. 29.	Dec. 6.	Dec. 13.	Dec. 20.	Dec. 27.	Jan. 3, 1891.	Jan. 10.	Jan. 17.	Jan. 24.	Jan. 31.
Diphtheria.....	57	81	84	97	86	81	120	114	94	105	95	90	103	107
Measles.....	108	131	183	141	236	238	269	319	253	298	390	413	453	433
Scarlet Fever....	53	58	65	65	79	93	69	86	108	113	154	134	146	174
Small-pox.....	...	1	...	1	1	...	...	...	...	...	...	...	...	...
Typhoid Fever...	30	27	21	25	16	23	21	12	9	16	8	7	10	13
Typhus Fever...	...	...	...	...	...	1	...	...	...	...	...	...	...	...
Total.....	248	298	353	329	418	436	479	531	464	532	647	644	712	727

Marriages reported	248	Burial permits issued	737
Births "	849	Transit permits issued	5
Deaths "	737	Searches made	256
Still-births "	65	Transcripts issued	204

Figure 1: Health Bulletin table reporting weekly cases of infectious diseases. See Appendix B for full page.

2.3.2 Vital Statistics, Volume 1: 1890–1899

Tables of the form shown in Figure 1 in volume 1 of the bulletins provide needed vital data where it could otherwise not be found.

2.3.3 Vital Statistics, Volume 1: 1898 Change in Reporting Area

The bulletin published for the week of Jan 15, 1898 was the first to include the larger reporting area mentioned previously. Vital statistics tables for that week and the one prior are shown in Figure 2 and Figure 3 to demonstrate the transition. Notice that though these consecutive bulletins occur in the same volume, their format changes to include data from the different boroughs.

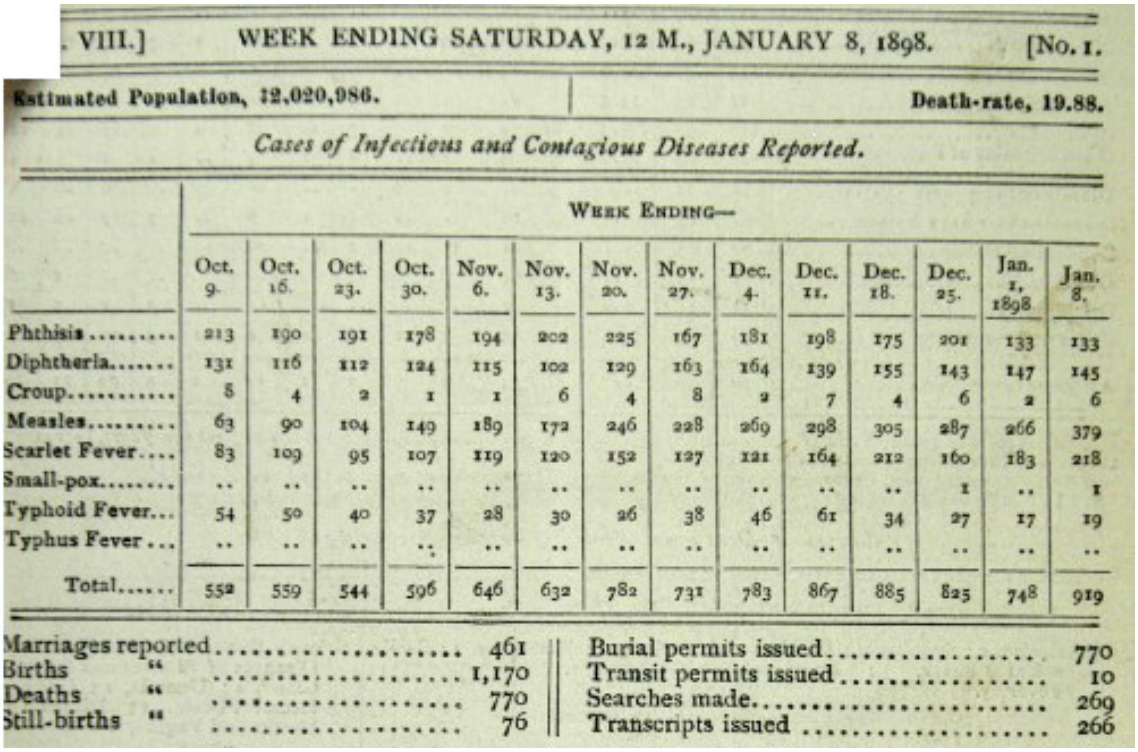

. VIII.] WEEK ENDING SATURDAY, 12 M., JANUARY 8, 1898. [No. 1.

Estimated Population, 12,020,986. **Death-rate, 19.88.**

Cases of Infectious and Contagious Diseases Reported.

	Week Ending—													
	Oct. 9.	Oct. 16.	Oct. 23.	Oct. 30.	Nov. 6.	Nov. 13.	Nov. 20.	Nov. 27.	Dec. 4.	Dec. 11.	Dec. 18.	Dec. 25.	Jan. 1, 1898	Jan. 8.
Phthisis.....	213	190	191	178	194	202	225	167	181	198	175	201	133	133
Diphtheria.....	131	116	112	124	115	102	129	163	164	139	155	143	147	145
Croup.....	8	4	2	1	1	6	4	8	2	7	4	6	2	6
Measles.....	63	90	104	149	189	172	246	228	269	298	305	287	266	379
Scarlet Fever....	83	109	95	107	119	120	152	127	121	164	212	160	183	218
Small-pox.....	..	..	..	..	..	..	..	..	..	..	..	1	..	1
Typhoid Fever...	54	50	40	37	28	30	26	38	46	61	34	27	17	19
Typhus Fever ...	..	..	..	..	..	..	..	..	..	..	..	..	..	..
Total.....	552	559	544	596	646	632	782	731	783	867	885	825	748	919

Marriages reported	461	Burial permits issued	770
Births "	1,170	Transit permits issued	10
Deaths "	770	Searches made.....	269
Still-births "	76	Transcripts issued	266

Figure 2: Health Bulletin table reporting vital statistics for only Manhattan Island, week of Jan. 8, 1898.

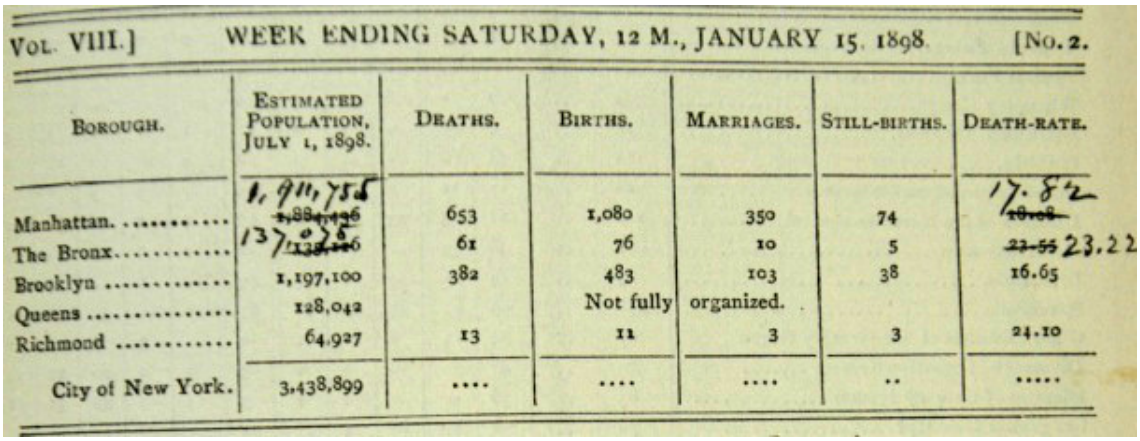

VOL. VIII.] WEEK ENDING SATURDAY, 12 M., JANUARY 15, 1898. [NO. 2.

BOROUGH.	ESTIMATED POPULATION, JULY 1, 1898.	DEATHS.	BIRTHS.	MARRIAGES.	STILL-BIRTHS.	DEATH-RATE.
Manhattan.....	1,911,758 ~~1,884,436~~	653	1,080	350	74	17.82 ~~18.08~~
The Bronx.....	137,035 ~~138,116~~	61	76	10	5	~~23.55~~ 23.22
Brooklyn	1,197,100	382	483	103	38	16.65
Queens	128,042		Not fully	organized.		
Richmond	64,927	13	11	3	3	24.10
City of New York.	3,438,899	....	....	....	..	.....

Figure 3: Health Bulletin table reporting vital statistics for Manhattan, The Bronx, Brooklyn, Queens, and Richmond, week of Jan 15, 1898. The hand corrections are uncommon in these documents; they are the result of Health Dept. reorganization.

2.3.4 Disease Incidence: 1915

Sometime between 1914 and 1916, the NYC Health Dept. adjusted the form of its bulletins, and the transitional year, 1915, presents some difficulty. Figure 4 shows the only available data tables regarding cases of reportable infectious diseases found for that year.

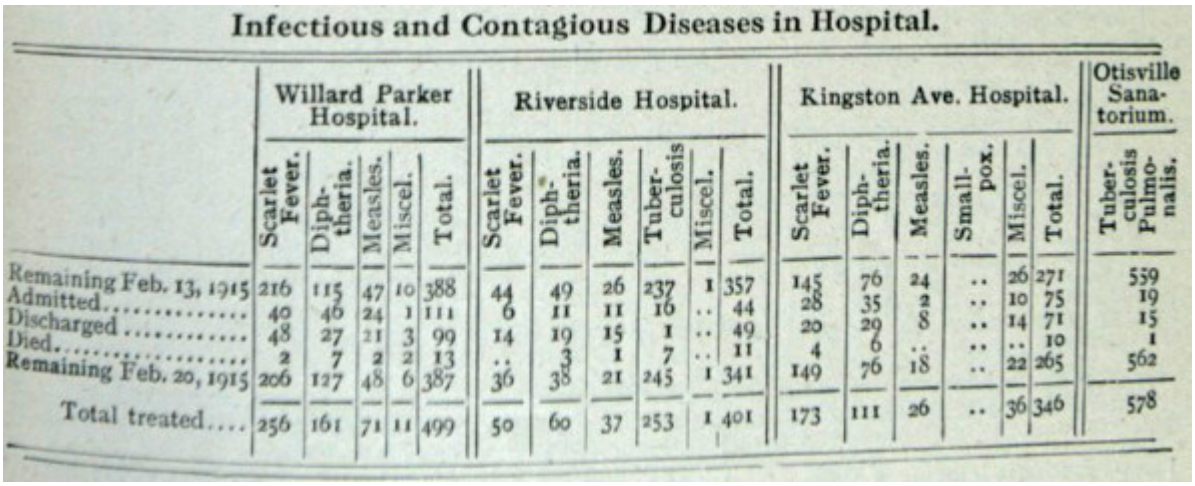

Infectious and Contagious Diseases in Hospital.

	Willard Parker Hospital.					Riverside Hospital.						Kingston Ave. Hospital.						Otisville Sanatorium.
	Scarlet Fever.	Diphtheria.	Measles.	Miscel.	Total.	Scarlet Fever.	Diphtheria.	Measles.	Tuberculosis	Miscel.	Total.	Scarlet Fever.	Diphtheria.	Measles.	Smallpox.	Miscel.	Total.	Tuberculosis Pulmonalis.
Remaining Feb. 13, 1915	216	115	47	10	388	44	49	26	237	1	357	145	76	24	..	26	271	559
Admitted	40	46	24	1	111	6	11	11	16	..	44	28	35	2	..	10	75	19
Discharged	48	27	21	3	99	14	19	15	1	..	49	20	29	8	..	14	71	15
Died	2	7	2	2	13	..	3	1	7	..	11	4	6	..	..	..	10	1
Remaining Feb. 20, 1915	206	127	48	6	387	36	38	21	245	1	341	149	76	18	..	22	265	562
Total treated	256	161	71	11	499	50	60	37	253	1	401	173	111	26	..	36	346	578

Figure 4: Health Bulletin table showing reportable infectious diseases, week of Feb. 20, 1915. See Appendix B for full page.

Notice that city-wide totals of cases are not reported. Instead measles cases are reported only for three hospitals within the city. These numbers are themselves not representative of the entire city, but fortunately we can re-sale them using an independent data source (see §2.6).

2.3.5 Disease Incidence, Volume 2: 1916–1932

The format of the tables from which disease incidence data were drawn changed slightly compared to the previous volume, and tables appeared as shown in Figure 5.

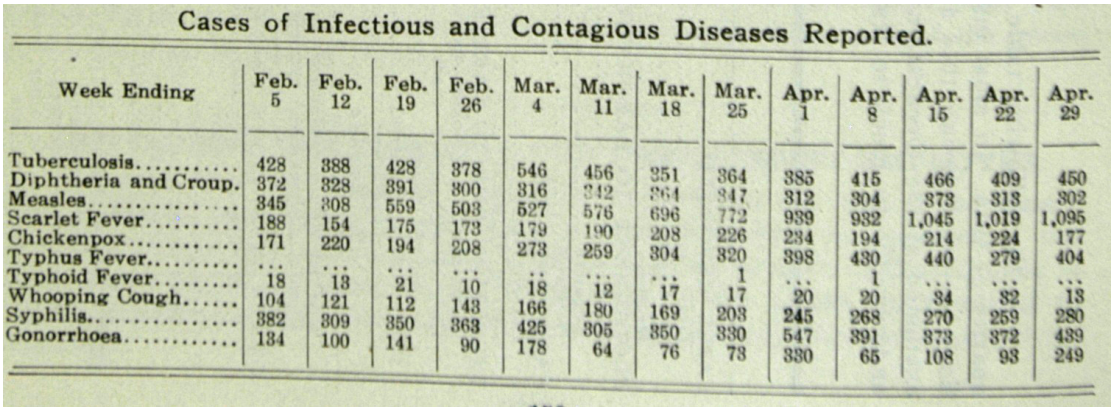

Cases of Infectious and Contagious Diseases Reported.

Week Ending	Feb. 5	Feb. 12	Feb. 19	Feb. 26	Mar. 4	Mar. 11	Mar. 18	Mar. 25	Apr. 1	Apr. 8	Apr. 15	Apr. 22	Apr. 29
Tuberculosis	428	388	428	378	546	456	351	364	385	415	466	409	450
Diphtheria and Croup.	372	328	391	300	316	342	364	347	312	304	373	313	302
Measles	345	308	559	503	527	576	696	772	939	932	1,045	1,019	1,095
Scarlet Fever	188	154	175	173	179	190	208	226	234	194	214	224	177
Chickenpox	171	220	194	208	273	259	304	320	398	430	440	279	404
Typhus Fever	...	...	...	...	..	...	...	1	...	1	...	...	...
Typhoid Fever	18	13	21	10	18	12	17	17	20	20	34	32	13
Whooping Cough	104	121	112	143	166	180	169	203	245	268	270	259	280
Syphilis	382	309	350	363	425	305	350	330	547	391	373	372	439
Gonorrhoea	134	100	141	90	178	64	76	78	330	65	108	93	249

Figure 5: Health Bulletin table reporting weekly cases of infectious diseases. See Appendix B for full page.

2.3.6 Tabulation

For the tables containing disease incidence rates in volumes 1 and 2, notice that for each week's bulletin, a full quarter-year of previous weeks' worth of reported cases are shown. This means that in order to extract a year's worth of data, no more than five sample bulletins are required. As a result, we did not photograph all Weekly Bulletin pages, but instead sampled pages periodically such that completely overlapping disease incidence tables were acquired. Notice that the table providing vital statistics shows only information for the week in question. For the total population of NYC at the time, this did not present a problem; weekly changes in population are not significant compared to the total population, we can therefore estimate a yearly average population from these numbers. Birth rates oscillate throughout the year [13], and so for years in which a full set of bulletin photographs had not been acquired, we use weekly data points available periodically throughout the year to estimate the yearly value.

2.4 Health Dept. Records 1958–1976 Weekly Disease Incidence Data

The NYC Health Department kept detailed records of the incidence of many diseases and conditions, including infectious diseases of interest to us. In particular, from 1958–1976, weekly records were kept of the incidence of diseases and conditions by health district of residence, of which there are 27 in NYC (this date range represents only what we were able to find, but all indications suggest that such data were

collected for a wider range of dates). These are organized by boroughs and city-wide totals are available for our purposes. See Figure 6 for a sample table providing city-wide totals, and Appendix B for a sample of a full weekly report.

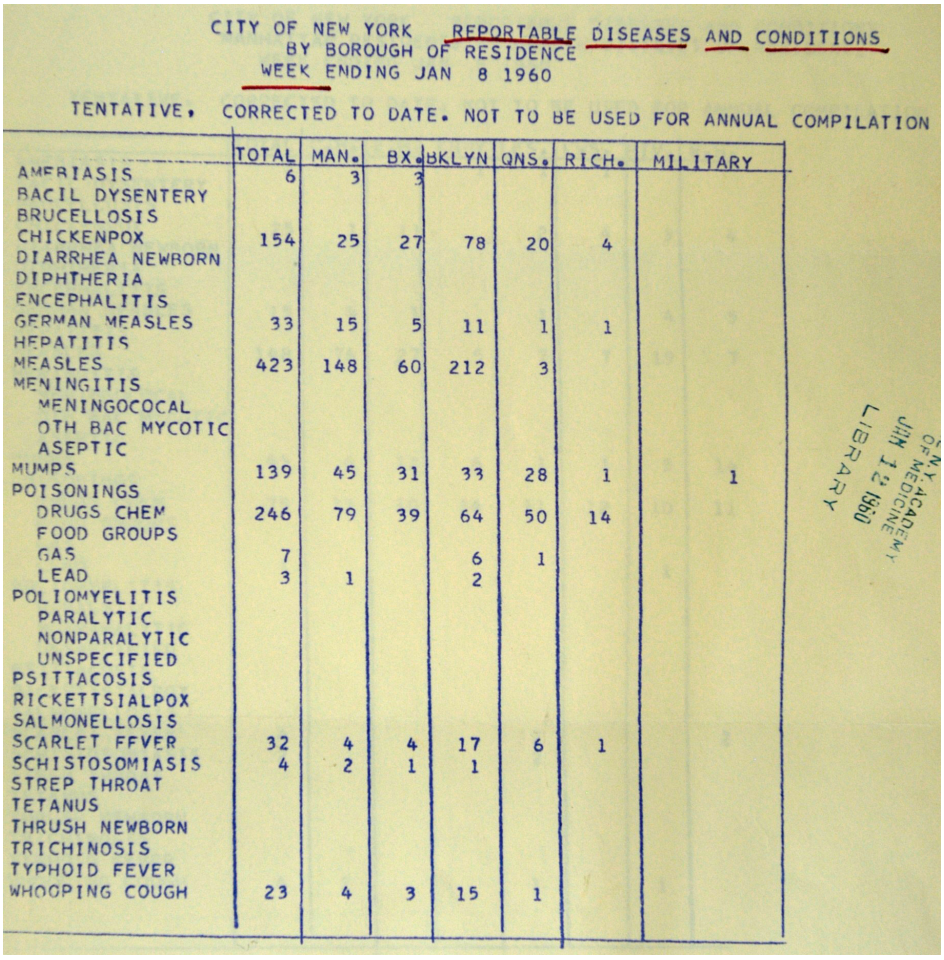

CITY OF NEW YORK REPORTABLE DISEASES AND CONDITIONS
BY BOROUGH OF RESIDENCE
WEEK ENDING JAN 8 1960

TENTATIVE, CORRECTED TO DATE. NOT TO BE USED FOR ANNUAL COMPILATION

	TOTAL	MAN.	BX.	BKLYN	QNS.	RICH.	MILITARY
AMEBIASIS	6	3	3				
BACIL DYSENTERY							
BRUCELLOSIS							
CHICKENPOX	154	25	27	78	20	4	
DIARRHEA NEWBORN							
DIPHTHERIA							
ENCEPHALITIS							
GERMAN MEASLES	33	15	5	11	1	1	
HEPATITIS							
MEASLES	423	148	60	212	3		
MENINGITIS							
MENINGOCOCAL							
OTH BAC MYCOTIC							
ASEPTIC							
MUMPS	139	45	31	33	28	1	1
POISONINGS							
DRUGS CHEM	246	79	39	64	50	14	
FOOD GROUPS							
GAS	7			6	1		
LEAD	3	1		2			
POLIOMYELITIS							
PARALYTIC							
NONPARALYTIC							
UNSPECIFIED							
PSITTACOSIS							
RICKETTSIALPOX							
SALMONELLOSIS							
SCARLET FEVER	32	4	4	17	6	1	
SCHISTOSOMIASIS	4	2	1	1			
STREP THROAT							
TETANUS							
THRUSH NEWBORN							
TRICHINOSIS							
TYPHOID FEVER							
WHOOPING COUGH	23	4	3	15	1		

Figure 6: NYC Health Dept. table showing reportable diseases and conditions. See Appendix B for full weekly report.

2.5 NYC Health Dept. Vital Statistics Reports: 1900–1984

The NYC Health Dept. website has made historical vital statistics reports available to the general public [1]. These reports, for the years of 1976–1984, contain tables showing city-wide monthly aggregated cases of reportable diseases. For years outside

of this range and going back to 1950, yearly aggregated data is provided in the reports we obtained. For disease incidence, yearly data is by no means sufficient for our purposes. However, these vital statistics reports, as the name would imply, contain vital data, for which yearly numbers are adequate. Furthermore, 5-year aggregated totals are reported from 1900–1950.

2.6 1915

We noted previously that we must further discuss the Weekly Bulletin data for the year 1915. Disease incidence numbers prior to 1915 come from Volume 1 of the Health Bulletins, and after 1915 come from Volume 2, as noted previously. The data before and after 1915 represent measles cases for all of NYC, whereas the data we have for 1915 represent counts taken for only three hospitals within the city. Using yearly aggregated reported measles cases taken from the NYC Vital Statistics Reports [1] and comparing them with yearly totals from the Health Bulletin data (see Figure 9), we determine a scaling factor (5.04) with which to adjust the weekly Health Bulletin Data. Figure 7 shows measles incidence rates recorded for the years surrounding 1915 before we re-sale the 1915 data. We conclude from the apparent consistency in the pattern of outbreaks that the adjustment is appropriate.

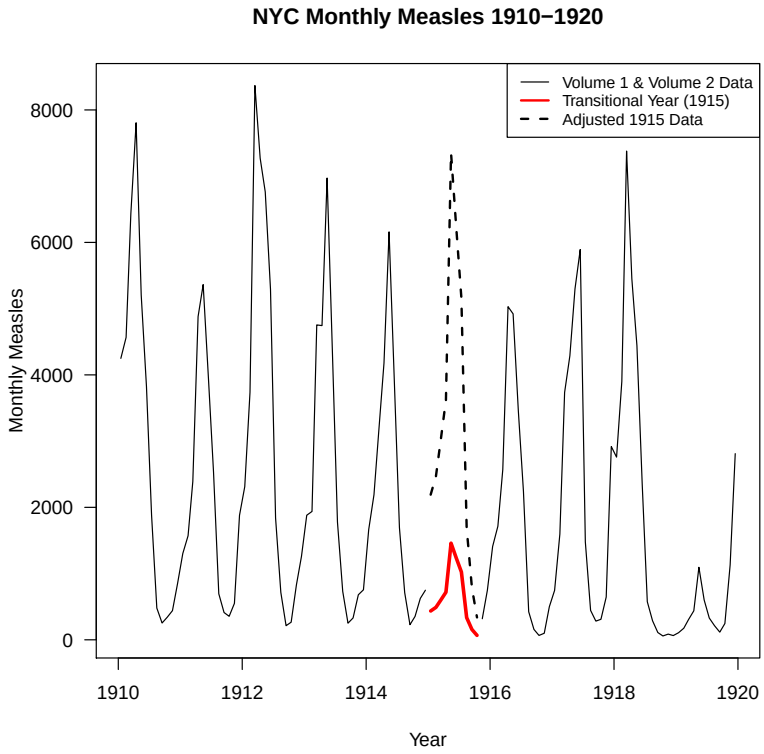

Figure 7: Time series plot of tabulated Health Bulletin data from 1910–1920, showing original and adjusted 1915 reported measles cases from three hospitals in the context of city-wide measles cases for other years.

2.7 Formatting the Data

For our analysis, we make use of weekly and monthly aggregated measles data, and yearly vital data. For large time spans (namely 1932–1958 and 1976–1984), we have only monthly data, hence we interpolate pseudo-weekly data from the monthly data points. To do this, we split the monthly total of cases between the weeks of the month, and then smooth the weekly values linearly, fixing the number of cases per week in the middle of each month. For vital statistics, we obtain yearly total population and birth rates from the NYC Health Bulletins for 1891–1900 as detailed previously §2.3.2, and from the NYC Dept. of Health vital statistics reports for 1900–1984. Note that the vital statistics reports contain only data points every 5 years

from 1900–1950, and so we interpolate yearly points linearly from these as well.

2.8 Summary of Available and Compiled Data

Since we are using data from various overlapping sources, we need to pick time points where we transition from one source to the next. Since it is better to do analyses using originally recorded weekly data rather than pseudo-weekly interpolation, we will use as much originally recorded weekly data as possible.

Data Available		
Data Source	Measles Incidence	Vital Statistics
Weekly Bulletins Vol 1 (Appendix B)	1891–1914 (W)	1891–1914 (Y)
Weekly Bulletins 1915 (Appendix B)	1915 (W)	N/A
Weekly Bulletins Vol 2	1916–1932 (W)	1916–1932 (Y)
London and Yorke [20]	1928–1972 (M)	N/A
Health Department Records	1958–1976 (W)	N/A
Vital Statistics Reports	1976–1984 (M)	1900–1950 (5Y) 1950–1984 (Y)

Table 1: Frequency of data points are shown as weekly (W), monthly (M), yearly (Y), or every 5 years (5Y).

Data Compiled		
Time Period	Measles Incidence	Vital Statistics
1891–1900	Weekly Bulletins Vol 1	Weekly Bulletins Vol 1
1900–1914	Weekly Bulletins Vol 1	Vital Statistics Reports
1915	Weekly Bulletins 1915	Vital Statistics Reports
1916–1932	Weekly Bulletins Vol 2	Vital Statistics Reports
1932–1958	London and Yorke [20]	Vital Statistics Reports
1958–1976	Health Department Records	Vital Statistics Reports
1976–1984	Vital Statistics Reports	Vital Statistics Reports

Table 2: Components of sources compiled into a continuous times series.

2.9 Normalized Data

For our analysis of the disease incidence data, we need to control for changes in population size. To this end we have constructed a time-series of yearly total population numbers, as detailed previously. Using the population data, we can normalize disease incidence data with respect to population size. This serves to remove elements of the dynamics which are simply artifacts of changes in population, and what remains is a more consistent representation of the dynamics of measles. See Figure 8 for a plot of total population with respect to time, which we use to normalize our data. Note in particular the high rate of population growth in the early 1900s; much of an apparent rise in measles incidence can be attributed to this. The sudden jump in the population data is attributed to a change in reporting area (see §2.3)

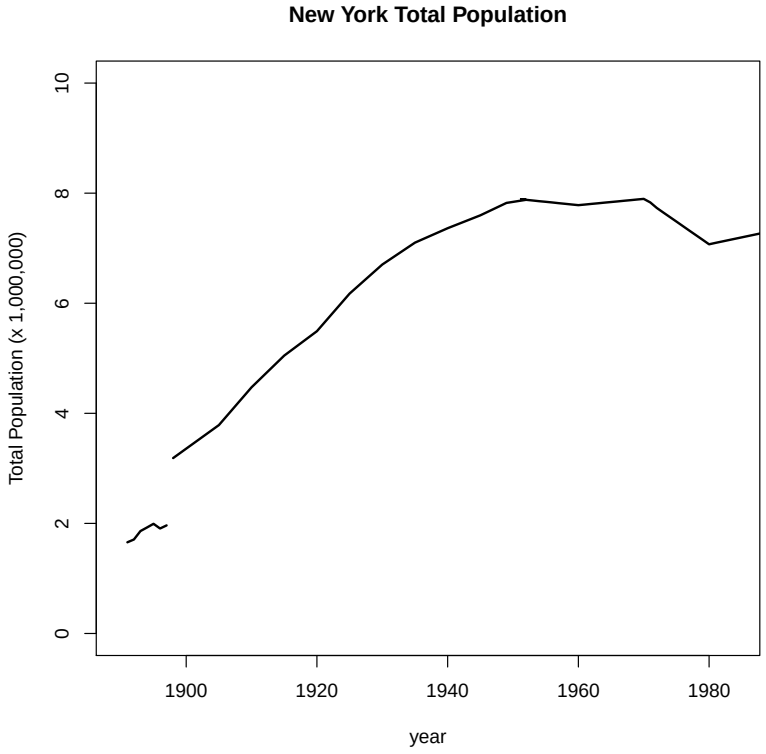

Figure 8: Time series plot of the total population of NYC from 1891–1984.

2.10 Sanity Checks

Since much of the data we use is from original digitization, it is appropriate to conduct a number of checks on the data to ensure that its quality is acceptable for the analysis. We therefore cross-reference our new data with as much independent information as we can. To this end we perform the following three sanity checks on our new data:

1. The NYC Health Department Vital Statistics Reports [1] list yearly totals for disease incidence from 1911 to the present. Our first check takes yearly sums of our weekly data from the Health Bulletins in the timespan of 1911–1932, and compares these yearly sums to data from the Health Department Vital Statistics Reports. See Figure 9 for this comparison. We conclude that, with the exception of the year 1915 (which we dealt with previously), the close match of these totals evidences reliability of the Health Bulletin data.

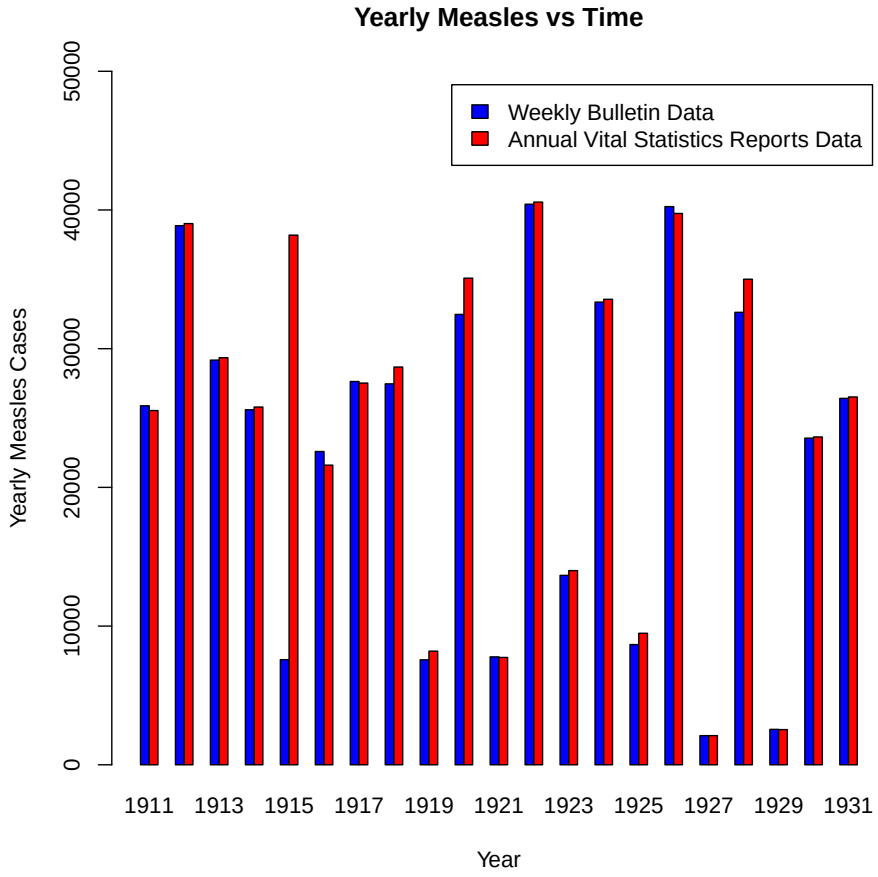

Figure 9: Overlapping time series plots of yearly measles incidence counts taken from the Health Bulletins and the Health Dept. Vital Statistics Reports.

2. Much of the newly digitized data overlaps with monthly data previously published by London and Yorke [20]. We can therefore use monthly tabulated totals of our original weekly data in the overlapping periods and compare them to London and Yorke's data. The results of this second check are shown in Figures 10 and 11. Interestingly, these numbers do not match up perfectly, suggesting that adjustments were made by the NYC Health Department to the data we acquired (both from the Health Bulletins and the Health Department Records), prior to its tabulation in the paper published in 1973 by London and

Yorke [20].[2] The monthly sums of measles cases, however, match up closely enough in both overlapping time periods that we conclude our weekly data are reliable.

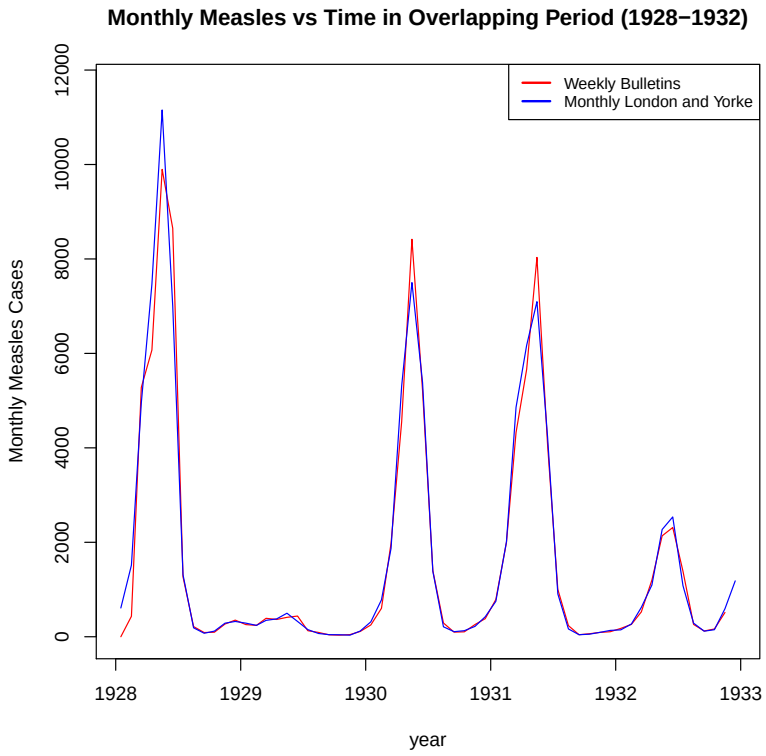

Figure 10: Overlapping time series plots of London and Yorke's monthly measles incidence rates, and the Health Dept. Bulletins weekly measles incidence rates, from 1928–1932. To compare these numbers, we have summed the weekly Bulletin data monthly, summing up the number of measles cases reported at the ends of weeks that fall in the same month.

[2]London and Yorke give very little information regarding the source of the data published their 1973 paper [20], only mentioning that the provider was the NYC Health Dept. Bureau of Infectious Disease Control (which no longer exists)

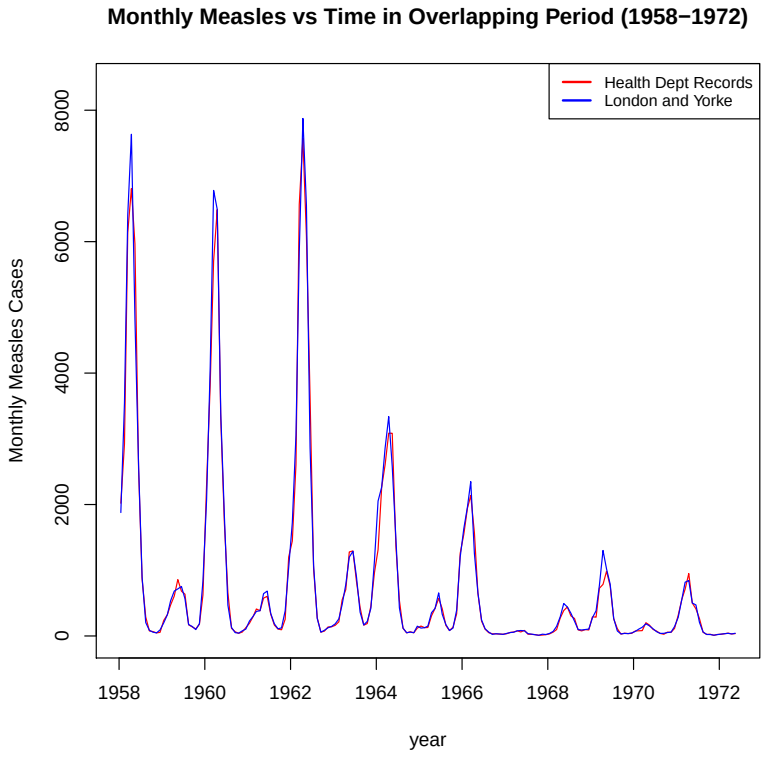

Figure 11: Overlapping time series plots of London and Yorke's monthly measles incidence rates, and the Health Dept. Records weekly incidence rates summed monthly, from 1958–1973.

3 Analysis

In this section we describe the statistical and analytic tools we use to examine measles dynamics in NYC. We begin with a delineation of the SIR model, and describe how we use $\mathcal{R}_{0,\text{eff}}$ (see §3.1) as a predictor for the frequency structure of measles in NYC. We then use demographic data from NYC to estimate values of $\mathcal{R}_{0,\text{eff}}$ for each year in our range of dates from 1891–1984, and use the resulting time-series of $\mathcal{R}_{0,\text{eff}}$ to predict the frequency structure of measles in NYC throughout this time period. Using a continuous wavelet transform, we plot the actual frequency structure of the observed time series and overlay the predicted frequency structure for comparison (see Figure 13).

3.1 The SIR Model

Krylova and Earn [19] have previously used the SIR model to study the dynamics of measles in NYC, based on London and Yorke's data (1928–1973). As a result, much work regarding numerous aspects of our undertaking has already been done. Most importantly, we already have access to good estimates of all model parameters, and we use the same method as Krylova and Earn for the estimation of $\mathcal{R}_{0,\text{eff}}$ at different times during the time-series (see Equation (5)). More realistic (and complicated) versions of the model exist. However, Krylova and Earn [19] showed that the dynamics of the model (when properly parameterized) are almost identical to the dynamics of models with multiple stages of infection with realistically distributed durations. The compartments of the SIR model, S, I, and R represent the individuals in a population that are *Susceptible*, *Infected*, and *Recovered*, respectively. The following system of ODEs represents the flow rates from one compartment to the next:

$$\frac{dS}{dt} = \Phi - \beta SI - \mu S \tag{1a}$$

$$\frac{dI}{dt} = \beta SI - \gamma I - \mu I \tag{1b}$$

$$\frac{dR}{dt} = \gamma I - \mu R \tag{1c}$$

Notice that individuals remain in the recovered state after they have entered it. This is consistent with the behaviour of diseases like measles, to which lifelong immunity is acquired after first infection. The parameters β, μ, γ represent the rates of transmission, *per capita* death, and recovery, respectively. μ represents the rate of death from natural causes, and deaths resulting from infection are assumed to be negligible. Φ represents the birth rate, and varies with time. $N = S + I + R$ is the total population size, which remains fixed if $\Phi = \mu N$, in which case births would balance deaths. We do not assume this, however, because secular changes in Φ can cause dynamical transitions [5, 6, 10, 11, 19]. Instead, we estimate Φ from demographic data for NYC. The expression for the incidence, βSI, makes the assumption that the population being studied is well mixed; all individuals infect one another at the same rate, and this rate is given by β. This assumption of mixing is generally a good one for populations confined to a small geographic area, namely cities. Equations (1a) and (1b) do not depend on Equation (1c), so the latter can be ignored. We derive a normalized birth rate ν by relating real birth counts of the NYC population to concurrent total population estimates. For the population size N_0 at time t_0, we write $\Phi = \nu N_0$ such that ν is the *per capita* birth rate at exactly time t_0. The system of equations then

becomes:

$$\frac{dS}{dt} = \nu N_0 - \beta SI - \mu S \tag{2a}$$
$$\frac{dI}{dt} = \beta SI - \gamma I - \mu I \tag{2b}$$
$$\frac{dR}{dt} = \gamma I - \mu R \tag{2c}$$

Technically speaking, we should be referring to ν as the *per capita* rate of recruitment of susceptible individuals into the population, rather than the birth rate. This distinction, however, is only relevant if not all births result in susceptible individuals entering the population, and as a result we must consider vaccinations kedit(in principle immigration can also be a source of new susceptibles, but at such a low rate compared to the NYC birth rate that it is insignificant). We make reference to ν with the understanding that discrepancies between the birth rate and the rate of susceptibles entering the population will be dealt with explicitly. Additionally, we note that immigration does not significantly impact measles dynamics in NYC, since immigrating infectives are only relevant in preventing disease fadeouts in small populations, and the NYC population is too large for this to be an issue. As we move forward, we will be making reference to a fundamental characteristic of an infectious disease, the *basic reproduction number* $\mathcal{R}_0$. This number represents, for a given disease, the average number of new infections that result from a single infected individual in a completely susceptible population [4]. Theoretically, if its $\mathcal{R}_0 < 1$, the disease cannot sustain itself in a population and will die out, and if $\mathcal{R}_0 > 1$ it can spread. For the SIR model,

$$\mathcal{R}_0 = \frac{\nu N_0}{\mu} \frac{\beta}{\gamma + \mu} \tag{3}$$

[19] The factor $(\frac{\nu N_0}{\mu})$ is included in the expression for $\mathcal{R}_0$ because we did not define $\Phi = \nu N$, and instead use real demographic data to estimate ν. We assume that the birth rate ν changes slowly enough that $\mathcal{R}_0$ can be defined at a given time taking ν as a constant.

3.2 Seasonal Transmission Rate

A very typical addition to infectious disease models is *seasonal forcing* [10,11,20,22], and in our instantiation of the SIR model this is introduced into the transmission rate β. The reason for introducing this added complexity was discussed in §1.1:

contact between individuals varies seasonally. In particular, contact among the most likely individuals to be infected or susceptible—namely children—increases drastically during the school term. Seasonal variation can also be modeled in the birth rate, however He and Earn [13] showed that for the SIR model parameterized for measles, seasonal variation in the birth rate does not significantly impact dynamics. Seasonal forcing is usually introduced into the SIR model in one of two ways, sinusoidal forcing or term-time forcing [16]. Both of these methods change the parameter β into a seasonally varying function of time $\beta(t)$. Term-time forcing assigns either a high or a low value to $\beta(t)$ according to the time of year when school is in session. Sinusoidal forcing treats $\beta(t)$ as a continuous function of time:

$$\beta(t) = \beta_0(1 + \alpha \cos(2\pi t)), \tag{4}$$

where β_0 is the mean transmission rate and α is the amplitude of forcing. In either case, the period of the forcing function is one year. Krylova and Earn [19] showed that for the simple version of the SIR model which we make use of, dynamics are virtually equivalent using either term-time or sinusoidal forcing (with different α for each case). We use the latter since it is easier to implement. We remark that making β a seasonally oscillating function of time changes our expression for $\mathcal{R}_0$ (Equation (3)) slightly; Ma and Ma [21] showed that one can replace this β with the β_0 from Equation (4).

3.3 Transition Analysis

3.3.1 Effective $\mathcal{R}_0$

As noted previously, we generate predicted behaviour of measles in the NYC population from the SIR model. The parameter we use to predict the dynamics of the disease incidence time series is $\mathcal{R}_0$, which in the SIR model depends on the *per capita* susceptible recruitment rate (see Equation (3)). For some anchor time t_0 in the time series, we use an estimate of $\mathcal{R}_0$ for measles [3]. Then, using this anchor value of $\mathcal{R}_0$, we calculate changes in the effective value of this parameter over time as the rate of susceptible recruitment changes. We take ν to be time dependent: $\nu(t)$, where $\nu_0 = \nu(t_0)$ is the susceptible recruitment rate at our anchor time t_0. Our equation

[3]Estimating $\mathcal{R}_0$ is not trivial. It must be done for a particular city and disease at a particular point in time. Krylova and Earn [19] used a 1960 estimate from Anderson and May [4] for England and Wales of approximately 17, and assumed this value to be common with NYC at the same point in time. However, an estimate of $\mathcal{R}_0$ using data from NYC has not yet been produced.

for $\mathcal{R}_0$ therefore becomes a modified version of Equation (3):

$$\mathcal{R}_0 = \frac{\nu_0 N_0}{\mu} \frac{\beta_0}{\gamma + \mu} \tag{5}$$

This represents our $\mathcal{R}_0$ estimate at t_0, but at other times we will need an estimate of the effective $\mathcal{R}_0$, which we will refer to as $\mathcal{R}_{0,\text{eff}}$, and this varies with time. We give the following expression for $\mathcal{R}_{0,\text{eff}}$ based on the changing susceptible recruitment rate $\nu(t)$:

$$\mathcal{R}_{0,\text{eff}} = \frac{\nu(t) N_0}{\mu} \frac{\beta_0}{\gamma + \mu} \tag{6a}$$

$$= \frac{\nu(t)}{\nu_0} \frac{\nu_0 N_0}{\mu} \frac{\beta_0}{\gamma + \mu} \tag{6b}$$

$$= \frac{\nu(t)}{\nu_0} \mathcal{R}_0 \tag{6c}$$

3.3.2 Attractor and Transient Analysis

With a parameterized version of the SIR model one can generate predicted behaviour, and the type of behaviour with which we are concerned is frequency structure. The two methods we will use to determine the predicted frequency structure of our time-series are *attractor analysis* and *transient analysis* [6, 19], previously referred to as asymptotic and perturbation analysis, respectively. Attractor analysis identifies attractors in the model, along with their associated periods if they are periodic [8, 10, 11, 18]. Using the SIR model parameterized for measles, we use XPPAUT [12] to generate numerical solutions. From arbitrary initial conditions, and using $\mathcal{R}_0$ as a control parameter, we run each solution until invariant behaviour is reached. In our case we find cyclic attractors with periods resonating with the seasonal year. We determine a range of asymptotic behaviour of our parameterized SIR model by varying $\mathcal{R}_0$ over many values and identifying the attractor to which the system converges in each case. A stroboscopic map of each attractor is generated by sampling the system once per year (January 1st) once invariant behaviour is reached. Results of this analysis are plotted in a bifurcation diagram Figure 12. For a given value of $\mathcal{R}_0$, the period of the attractor to which the system converges is referred to as the *predicted resonant period*.

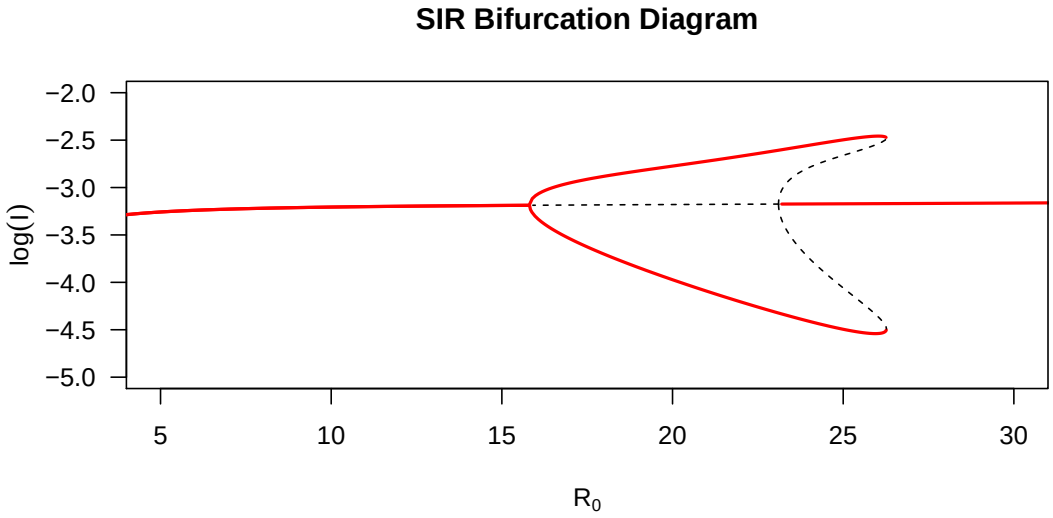

Figure 12: Asymptotic bifurcation diagram for measles in NYC. For each value of $\mathcal{R}_0$ on the x-axis, yearly values of the *Infected* SIR compartment are shown (on a log-scale, in red) from long term solutions of the system. When $\mathcal{R}_0 \lesssim 15.8$, an annual attractor is predicted (seen as a single red line on this plot). At $\mathcal{R}_0 \simeq 15.8$, there is a period doubling bifurcation. For $15.8 \lesssim \mathcal{R}_0 \lesssim 23.2$, a biennial attractor is predicted, since yearly levels of I alternate between a high and a low value. When $23.2 \lesssim \mathcal{R}_0 \lesssim 26.3$, both an annual and a biennial attractor are predicted. Long term solutions of the system will fall to one or the other, depending on initial conditions. For $26.3 \lesssim \mathcal{R}_0$ an annual attractor is once again predicted. Dashed lines show repellors, which can have important influences on dynamics [23]. Krylova [18, Fig. 7] showed that many higher period attractors exist for this parametrization of the SIR model, but their basins of attraction are small and they have not been observed in real world systems. Additionally, solutions locked onto these higher period attractors visit such low values of disease prevalence that they are very unlikely to exist in the NYC population. Finally, the seasonal forcing amplitude α has a significant impact on model dynamics, and we keep it fixed at 0.08 throughout our analysis (following Earn et al. [11] who studied who studied the NYC measles time-series for hte period 1928–1973). We revisit this issue later in §4.1.1.

For given values of $\mathcal{R}_0$, the system shows convergence to a cyclic attractor with a resonant period. However, the system of ODEs we integrate to determine this

fact are idealized; an infinite population size is assumed. In a finite population, demographic stochasticity is always present [6, 10]. Bauch and Earn also showed that if a system converges to the asymptotic attractor through damped transient oscillations, they have a very specific period depending on the value of $\mathcal{R}_0$. Since stochastic fluctuations prevent the system from reaching the asymptotic attractor, these transient oscillations are sustained [6], and as a result the system exhibits not only a resonant period, but also a non-resonant transient period sustained by stochasticity. For each cyclic attractor found in the previously described attractor analysis and over the same range of $\mathcal{R}_0$ values, one can linearize the system about the cycles in the associated stroboscopic map. For an attractor with period k, its transient period T_k is given by $\frac{2\pi k}{|Arg(\lambda_k)|}$, where λ_k is the dominant eigenvalue of the associated stroboscopic map [5, 6]. Following previous work [6, 19], we refer to this as the *predicted transient period*[4].

3.3.3 Wavelet Spectrum

In order to compare predicted resonant and transient periods from the SIR model with the frequency structure of our observed NYC measles data, we conduct a continuous wavelet transform on our NYC time-series of measles cases. A wavelet transform is similar to a Fourier decomposition: for some range of periods, it determines how prevalent each of these periods is in the time series by producing a power spectrum associated with each period. A wavelet transform, however, includes time as a variable in the decomposition: a power spectrum is produced for each period and for each point in time, giving the prevalence of periods as a function of time. Standard methods exist for doing this [3, 9, 24]. Results of the transform are typically summarized in a colour depth plot (See Figure 13, panel 3 for a colour depth plot of measles in NYC).

3.3.4 Analysis Summary

In conducting asymptotic and perturbation analysis on a parameterized version of the SIR model, we produce predicted resonant and transient periods for measles in NYC for the years 1891–1984. Predictions are largely based on estimates of $\mathcal{R}_{0,\text{eff}}$ at each point in time, and to produce these we use normalized yearly births from NYC

[4]Details on how to compute the resonant period with attractor analysis using the bifurcation analysis and continuation software XPPAUT [12] can be found in Krylova and Earn [19]. Computing the non-resonant period using perturbation analysis has also been done previously [6, 18], and note that the range of non-resonant periods we make use of in this paper are the same as those presented in Krylova [18, Fig. 5].

along with an estimate of $\mathcal{R}_0 = 17$ at the anchor time 1960, as well as vaccination data after 1963. We compare predicted periods in the time series with those observed in a continuous wavelet transform of the time-series of normalized weekly measles cases in NYC. Results are summarized in Figure 13

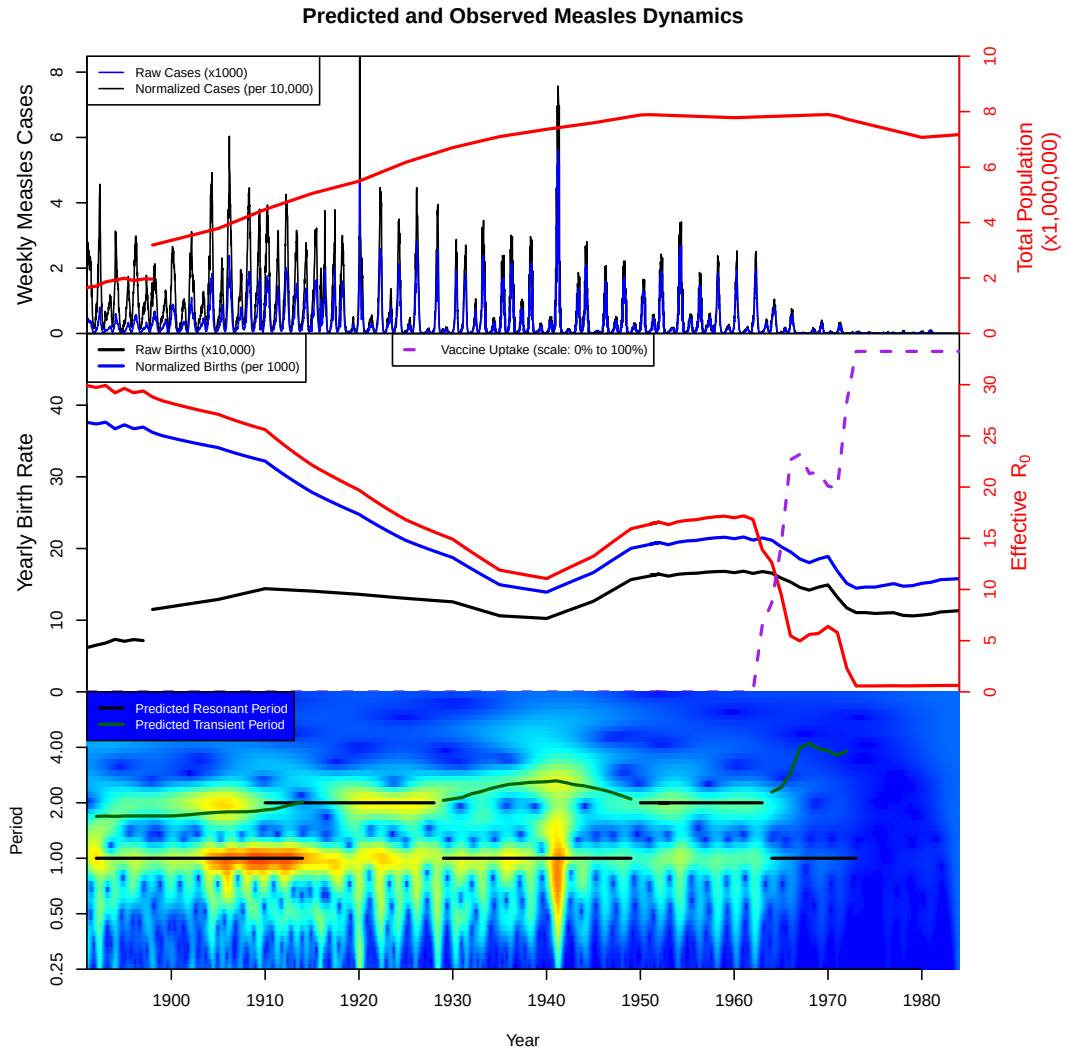

Figure 13: *Top panel, left axis:* Overlay of original weekly measles cases for 1891–1984 with normalized cases using yearly total population estimates. *Right axis:* Yearly total population. *Middle panel, left axis:* Overlaid raw yearly estimates of births with normalized births using total population estimates. Right axis: Estimates of $\mathcal{R}_{0,\text{eff}}$ used for analysis. Dotted line shows estimates of vaccine uptake. *Bottom panel:* Colour depth plot of a continuous wavelet transform of the normalized measles cases, where colour warmth scales with power. We have overlaid the predicted resonant and transient periods generated from analysis. Note that only the predicted transient period of the annual attractor appears in the spectral range shown in this diagram; the longer period attractors have much longer transient periods. [18].

4 Results

We now proceed with an examination of the results of our analysis, which are summarized in Figures 12 and 13, and we make reference to these throughout this section. We begin by dividing the time-series into intervals which appear to be separated by transitions in frequency structure. We then individually discuss each interval, along with the transitions that divide them, and compare predicted and observed behaviour. We list the following time intervals to this end, noting that the years given represent only the approximate locations of transitions:

- 1891–1910: Very high values of $\mathcal{R}_{0,\text{eff}}$ drive the predicted dynamics of the system to a region where only annual asymptotic behaviour is possible, $\mathcal{R}_0 > 26.3$. There is relatively good agreement between the predicted annual attractor and the power of the one-year period in this region, and we take this as the correct interpretation. What is puzzling, however, is the slight disagreement between the transient period predicted to be slightly below 2, and the observed power which seems to align itself exactly with a period of 2. The discrepancy is small, but it is possible that the annual attractor is incorrectly predicted, and that the system was locked in a biennial attractor in this period.

- 1910–1914: As $\mathcal{R}_{0,\text{eff}}$ continues to fall, the predicted dynamics enter the region in which both annual and biennial attractors are predicted. Either annual or biennial dynamics in the wavelet spectrum would be consistent with model predictions, noting that we would observe a non-resonant period near 2 if the real system was locked in an annual cycle. If our interpretation of the previous time interval is correct, then the latter is in fact the case, and we note that the transient period fades as we approach approximately 1914, a year in which we observe a transition in frequency structure.

- 1914–1929: Around 1914, we observe the high annual power in the wavelet spectrum transition into biennial power. Estimates of $\mathcal{R}_{0,\text{eff}}$ fall low enough that only a biennial attractor is predicted. If previous interpretations are correct, then the observed system falls off the annual attractor and lands on the biennial attractor. In other words, as $\mathcal{R}_{0,\text{eff}}$ decreases, the predicted model dynamics pass through a period-halving bifurcation at $\mathcal{R}_0 \approx 23.2$. This bifurcation divides the region where annual and biennial behaviour is possible from the region where only biennial behaviour is possible. In our interpretation, the disappearance of the annual attractor onto which the observed dynamics

appeared to have been locked causes the system to enter a period of hysteresis: convergence to the biennial attractor is not immediate, there is a time delay between when the system falls off of one attractor and lands on the other. The time delay is caused by the difference between prevalence, I, of a system locked onto the annual attractor just above the period halving bifurcation, and one locked onto a biennial attractor just below it. Strong agreement is found between the predicted biennial dynamics and the observed frequency structure in this time interval (note that biennial behaviour appears as both annual and biennial power in the wavelet spectrum).

- 1929–1950: We now move into a time interval which has been previously studied [19], but we will describe its contents for the sake of continuity. As $\mathcal{R}_{0,\text{eff}}$ continues to fall, predicted behaviour reaches a period-doubling bifurcation at $\mathcal{R}_0 \approx 15.8$, after which an annual attractor is predicted. Note that—unlike the transition described in the previous time interval—this transition of the system dynamics from biennial to annual is smooth, as one can see from the bifurcation diagram that the levels of I transition smoothly through the period-doubling bifurcation. The upshot is that we should observe an immediate shift in the system dynamics from biennial to annual. Observation is consistent with the system now being locked onto an annual attractor, as well as exhibiting a transient (non-resonant) period. In this region, $12 \leq \mathcal{R}_{0,\text{eff}} \leq 17$. As $\mathcal{R}_{0,\text{eff}}$ drops to a low near 1940, and rises again, we observe excellent agreement between the predicted transient period and high power in the wavelet spectrum.

- 1950–1964: $\mathcal{R}_{0,\text{eff}}$ continues to rise through 1950, but slows its rate of increase and remains at approximately 17 for the duration of this time interval. These values of $\mathcal{R}_{0,\text{eff}}$ place the predicted dynamics just to the right of the period-doubling bifurcation at $\mathcal{R}_0 \approx 15.8$, and so the SIR model predicts a biennial attractor. We observe both period 1 and period 2 power in the wavelet spectrum, which—as previously noted—is how a system locked in a biennial cycle appears on a wavelet spectrum. We conclude that there is strong agreement between predicted and observed dynamics.

- 1964–1984: As noted in §1.1, measles vaccination was introduced into the NYC population in 1964, and as uptake increased thereafter, overall measles cases decreased. Near the end of this time interval, the total number of measles cases

per unit time are small enough that stochasticity becomes very important, and a stochastic model is required to fully understand the observed dynamics. That being the case, annual power is still observed briefly at the start of this time interval, which is consistent with the predicted annual attractor for $\mathcal{R}_0 \leq 15.8$.

4.1 Comparing Predicted to Observed Periods

4.1.1 Resonant Period

There is very good agreement between predicted and observed resonant periods throughout the time-series we have studied. The only time interval in which agreement is less than perfect is 1891–1910, where—as noted previously—the predicted transient period does not precisely match the observed second peak of power in the wavelet spectrum. This discrepancy suggests, in the worst case, that our prediction is wrong and there is actually a biennial attractor, or in the better case that the predicted transient period is underestimated by $\sim 10\%$. In either case, it is likely that the parameterization of the SIR model is not precisely correct in this time interval. It is not clear which parameter requires attention, however several suggestions present themselves as most plausible. Values of the time dependent parameter $\mathcal{R}_{0,\text{eff}}$ were generated from an estimate of $\mathcal{R}_0$ for measles in England and Wales at anchor time $t_0 = 1960$. An estimate of $\mathcal{R}_0$ for measles in NYC in the early part of the 20th century would be very helpful in elucidating the issue with the SIR model parameterization early in our time-series. Without such an estimate on hand, however, we can speculate as to the source of the discrepancy between prediction and observation noted previously. In the definition of $\mathcal{R}_0$ found in Equation (3), consider only the factor $\frac{\beta}{\gamma+\mu}$ (the first factor concerns our estimation of $\mathcal{R}_{0,\text{eff}}$ from an anchor value). μ is small with respect to γ, and thus we can consider $\mathcal{R}_0 \approx \frac{\beta}{\gamma}$ and speculate as to why estimating $\mathcal{R}_{0,\text{eff}}$ from an anchor time in 1960 may be problematic near 1900. The recovery rate, γ, is characteristic of measles and does not change in the timespan we are dealing with. The transmission rate, β, varies seasonally with time with amplitude α and average β_0. As noted in §1.1, the seasonality of measles derives in large part from the pattern of school terms, which causes an increase in contact in the winter. Methods exist for fitting $\alpha(t)$ through the whole time series (rather than taking it to be constant),and may improve agreement between prediction and observation [15, 18].

4.1.2 Transient Period

Bauch and Earn [6, Fig. 3] present a plot comparing predicted transient periods to those observed in various time-series and for various diseases. We produce a similar plot to show the same relationship derived from our analysis of measles in NYC (see Figure 14).

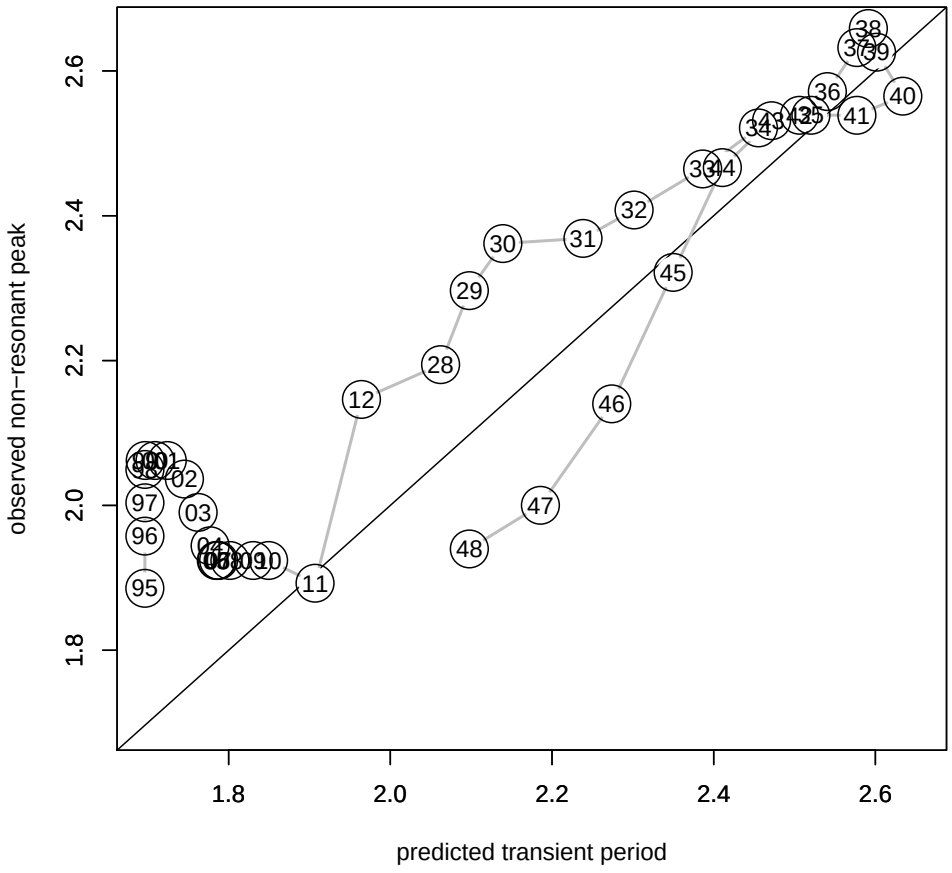

Figure 14: For all intervals of time in the span 1891–1984 for which an annual attractor is predicted, we find high spectral power at period 1, and a second spectral peak at some higher period (see Figure 13). For each such year, we determine the location of the second spectral peak in the wavelet spectrum (plotted on the y-axis) and compare with the concurrent predicted transient period (plotted on the x-axis). For each data point, the last two digits of the associated year are shown in the figure. The plotted line is $y{=}x$ (observation=prediction), not a fitted linear regression.

5 Conclusion

In light of the usefulness of NYC measles incidence data published in 1973 by London and Yorke [6, 8, 10, 20, 22], we extended the dataset to more than twice its previous length (1891–1984), adding large spans of higher quality (weekly rather than monthly) data. Concurrent demographic data was compiled for use in analysis, namely birth and total population numbers, aggregated yearly. We performed sanity checks on the new data we added to the time-series and verified its quality, making a few adjustments where needed.

We continued previous work done using the SIR model to understand measles dynamics in NYC [10, 19], using $\mathcal{R}_{0,\text{eff}}$ as a predictor for dynamical transitions. We obtained estimated values of $\mathcal{R}_{0,\text{eff}}$ throughout the years 1891–1984 using the rate of susceptible recruitment in NYC determined form birth rates and vaccine uptake. We used a continuous wavelet transform on the normalized time-series of measles incidence to observe its time-dependent frequency structure, and compared this with predicted SIR behaviour using $\mathcal{R}_{0,\text{eff}}$ values obtained from demographic data (Figure 13).

With the exception of periods of time near the beginning and end of our time-series, there is excellent agreement between SIR model predictions and observation. We attribute the slight disagreement early in the time-series to a need to fit the seasonal forcing amplitude $\alpha(t)$ throughout the time series. Very late in the time-series, stochastic simulation is required to fully understand the observed dynamics, as total measles cases per unit time fall drastically in response to high vaccine uptake. In our interpretation of the dynamical transitions, we find hysteresis—previously unobserved for measles in NYC—in the first half of our time-series. It should be noted that our interpretations of measles dynamics in NYC thus far have been based on analysis of the deterministic SIR model. In addition to further work examining the extremities of our newly extended time-series, future research should also quantitatively examine the relative powers of concurrent resonant and non-resonant spectral peaks using stochastic analysis [6, 7].

Appendix A Scripting and Programming Languages

Current work was done in "R" version 2.12.1.
To compute our continuous wavelet transform, we used an unpublished "R" package, "WaveletPackage_2.0.R", written by Michael Johansson [3]. Other "R" packages used include the following:

- "sfsmisc"
- "animation"
- "demography"
- "fields"

Appendix B Sample Photographs from Data Sources

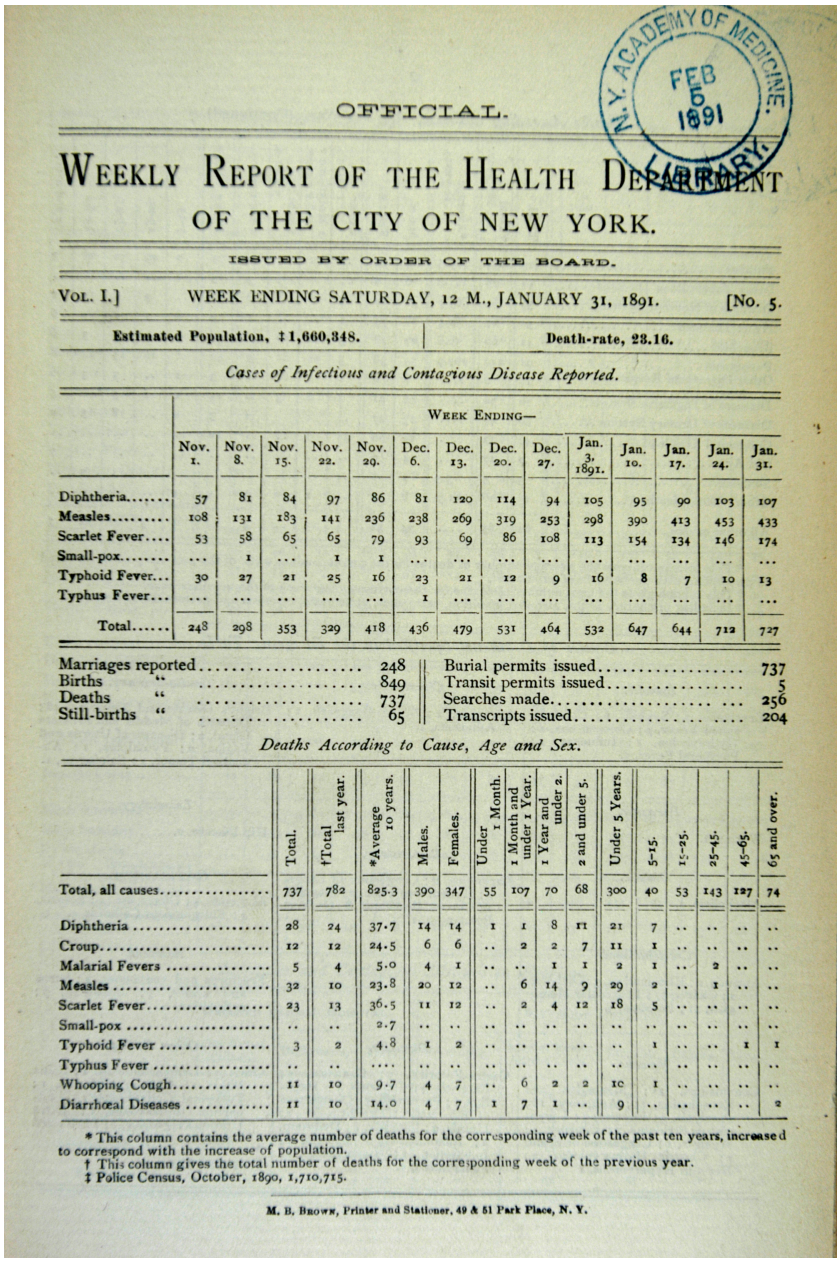

OFFICIAL.

WEEKLY REPORT OF THE HEALTH DEPARTMENT OF THE CITY OF NEW YORK.

ISSUED BY ORDER OF THE BOARD.

VOL. I.] WEEK ENDING SATURDAY, 12 M., JANUARY 31, 1891. [No. 5.

Estimated Population, ‡1,660,348. | **Death-rate, 23.16.**

Cases of Infectious and Contagious Disease Reported.

	Week Ending—													
	Nov. 1.	Nov. 8.	Nov. 15.	Nov. 22.	Nov. 29.	Dec. 6.	Dec. 13.	Dec. 20.	Dec. 27.	Jan. 3, 1891.	Jan. 10.	Jan. 17.	Jan. 24.	Jan. 31.
Diphtheria	57	81	84	97	86	81	120	114	94	105	95	90	103	107
Measles	108	131	183	141	236	238	269	319	253	298	390	413	453	433
Scarlet Fever	53	58	65	65	79	93	69	86	108	113	154	134	146	174
Small-pox	...	1	...	1	1	...	...	...	...	...	...	...	...	...
Typhoid Fever	30	27	21	25	16	23	21	12	9	16	8	7	10	13
Typhus Fever	...	...	...	...	...	1	...	...	...	...	...	...	...	...
Total	248	298	353	329	418	436	479	531	464	532	647	644	712	727

Marriages reported	248	Burial permits issued	737
Births "	849	Transit permits issued	5
Deaths "	737	Searches made	256
Still-births "	65	Transcripts issued	204

Deaths According to Cause, Age and Sex.

	Total.	†Total last year.	*Average 10 years.	Males.	Females.	Under 1 Month.	1 Month and under 1 Year.	1 Year and under 2.	2 and under 5.	Under 5 Years.	5-15.	15-25.	25-45.	45-65.	65 and over.
Total, all causes	737	782	825.3	390	347	55	107	70	68	300	40	53	143	127	74
Diphtheria	28	24	37.7	14	14	1	1	8	11	21	7	..	..	..	..
Croup	12	12	24.5	6	6	..	2	2	7	11	1	..	..	..	..
Malarial Fevers	5	4	5.0	4	1	..	..	1	1	2	1	..	2	..	..
Measles	32	10	23.8	20	12	..	6	14	9	29	2	..	1	..	..
Scarlet Fever	23	13	36.5	11	12	..	2	4	12	18	5	..	..	..	..
Small-pox	..	..	2.7	..	..	..	..	..	..	..	..	..	..	..	..
Typhoid Fever	3	2	4.8	1	2	..	..	..	..	..	1	..	..	1	1
Typhus Fever	..	..	....	..	..	..	..	..	..	..	..	..	..	..	..
Whooping Cough	11	10	9.7	4	7	..	6	2	2	10	1	..	..	..	..
Diarrhœal Diseases	11	10	14.0	4	7	1	7	1	..	9	..	..	..	..	2

* This column contains the average number of deaths for the corresponding week of the past ten years, increased to correspond with the increase of population.
† This column gives the total number of deaths for the corresponding week of the previous year.
‡ Police Census, October, 1890, 1,710,715.

M. B. Brown, Printer and Stationer, 49 & 51 Park Place, N. Y.

Figure 15: Weekly Bulletins Vol 1: Page 1

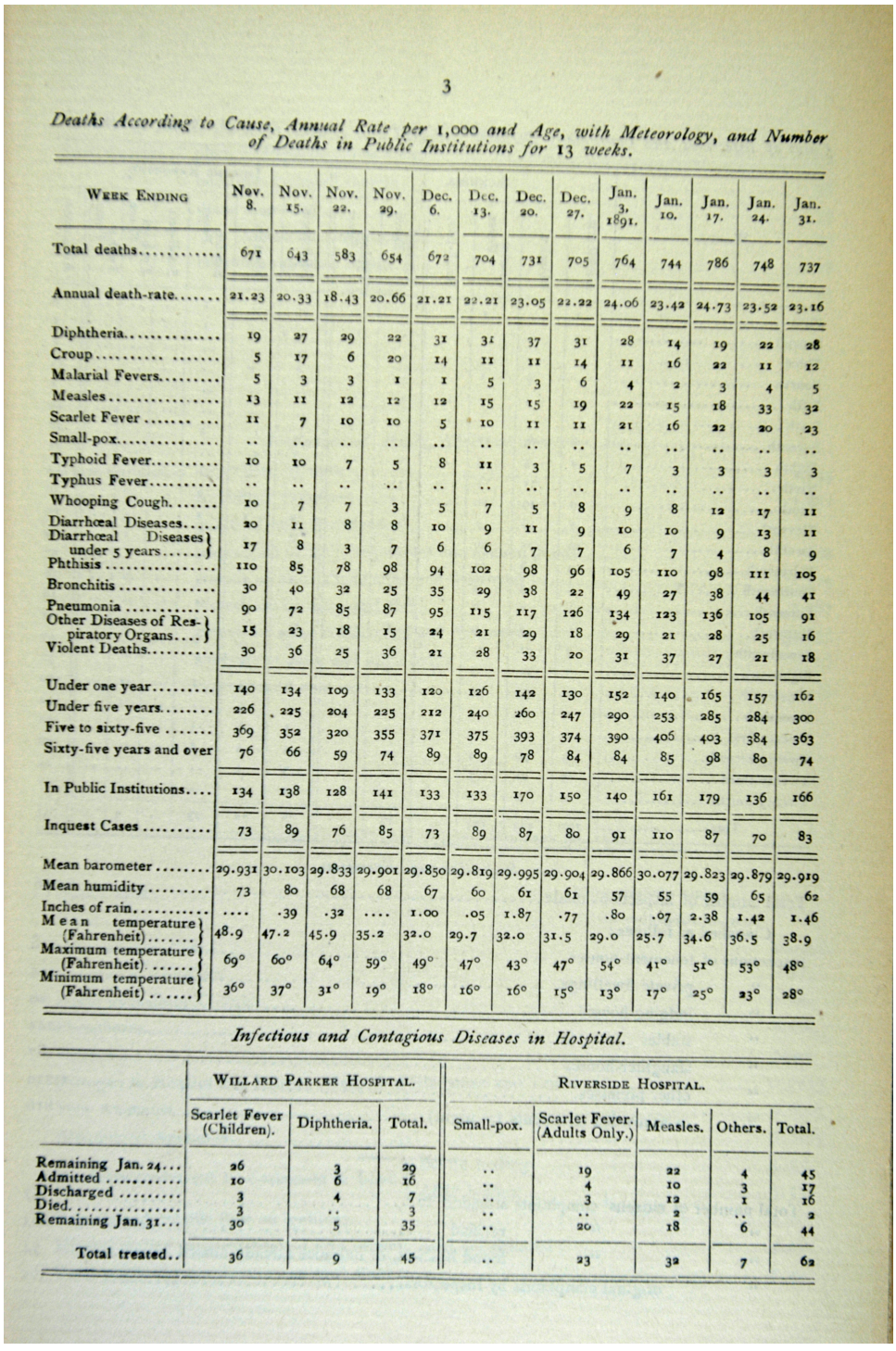

3

Deaths According to Cause, Annual Rate per 1,000 and Age, with Meteorology, and Number of Deaths in Public Institutions for 13 weeks.

Week Ending	Nov. 8.	Nov. 15.	Nov. 22.	Nov. 29.	Dec. 6.	Dec. 13.	Dec. 20.	Dec. 27.	Jan. 3, 1891.	Jan. 10.	Jan. 17.	Jan. 24.	Jan. 31.
Total deaths	671	643	583	654	672	704	731	705	764	744	786	748	737
Annual death-rate	21.23	20.33	18.43	20.66	21.21	22.21	23.05	22.22	24.06	23.42	24.73	23.52	23.16
Diphtheria	19	27	29	22	31	31	37	31	28	14	19	22	28
Croup	5	17	6	20	14	11	11	14	11	16	22	11	12
Malarial Fevers	5	3	3	1	1	5	3	6	4	2	3	4	5
Measles	13	11	12	12	12	15	15	19	22	15	18	33	32
Scarlet Fever	11	7	10	10	5	10	11	11	21	16	22	20	23
Small-pox	..	..	..	..	..	..	..	..	..	..	..	..	..
Typhoid Fever	10	10	7	5	8	11	3	5	7	3	3	3	3
Typhus Fever	..	..	..	..	..	..	..	..	..	..	..	..	..
Whooping Cough	10	7	7	3	5	7	5	8	9	8	12	17	11
Diarrhœal Diseases	20	11	8	8	10	9	11	9	10	10	9	13	11
Diarrhœal Diseases under 5 years	17	8	3	7	6	6	7	7	6	7	4	8	9
Phthisis	110	85	78	98	94	102	98	96	105	110	98	111	105
Bronchitis	30	40	32	25	35	29	38	22	49	27	38	44	41
Pneumonia	90	72	85	87	95	115	117	126	134	123	136	105	91
Other Diseases of Respiratory Organs	15	23	18	15	24	21	29	18	29	21	28	25	16
Violent Deaths	30	36	25	36	21	28	33	20	31	37	27	21	18
Under one year	140	134	109	133	120	126	142	130	152	140	165	157	162
Under five years	226	225	204	225	212	240	260	247	290	253	285	284	300
Five to sixty-five	369	352	320	355	371	375	393	374	390	406	403	384	363
Sixty-five years and over	76	66	59	74	89	89	78	84	84	85	98	80	74
In Public Institutions	134	138	128	141	133	133	170	150	140	161	179	136	166
Inquest Cases	73	89	76	85	73	89	87	80	91	110	87	70	83
Mean barometer	29.931	30.103	29.833	29.901	29.850	29.819	29.995	29.904	29.866	30.077	29.823	29.879	29.919
Mean humidity	73	80	68	68	67	60	61	61	57	55	59	65	62
Inches of rain	....	.39	.32	....	1.00	.05	1.87	.77	.80	.07	2.38	1.42	1.46
Mean temperature (Fahrenheit)	48.9	47.2	45.9	35.2	32.0	29.7	32.0	31.5	29.0	25.7	34.6	36.5	38.9
Maximum temperature (Fahrenheit)	69°	60°	64°	59°	49°	47°	43°	47°	54°	41°	51°	53°	48°
Minimum temperature (Fahrenheit)	36°	37°	31°	19°	18°	16°	16°	15°	13°	17°	25°	23°	28°

Infectious and Contagious Diseases in Hospital.

	Willard Parker Hospital.			Riverside Hospital.				
	Scarlet Fever (Children).	Diphtheria.	Total.	Small-pox.	Scarlet Fever. (Adults Only.)	Measles.	Others.	Total.
Remaining Jan. 24	26	3	29	..	19	22	4	45
Admitted	10	6	16	..	4	10	3	17
Discharged	3	4	7	..	3	12	1	16
Died	3	..	3	..	..	2	..	2
Remaining Jan. 31	30	5	35	..	20	18	6	44
Total treated	36	9	45	..	23	32	7	62

Figure 16: Weekly Bulletins Vol 1: Page 2

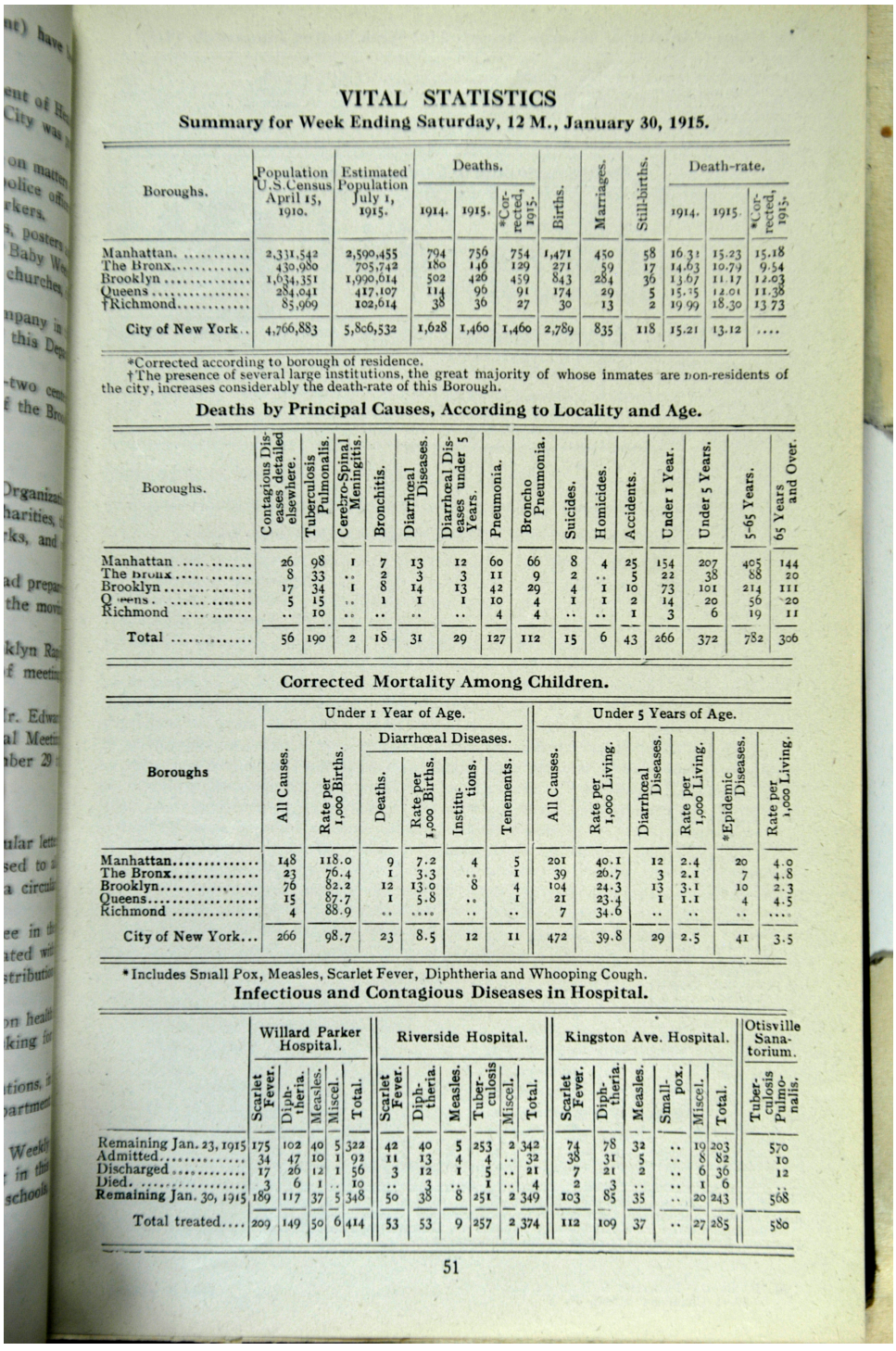

VITAL STATISTICS

Summary for Week Ending Saturday, 12 M., January 30, 1915.

Boroughs.	Population U.S.Census April 15, 1910.	Estimated Population July 1, 1915.	Deaths. 1914.	Deaths. 1915.	Deaths. *Corrected, 1915.	Births.	Marriages.	Still-births.	Death-rate. 1914.	Death-rate. 1915.	Death-rate. *Corrected, 1915.
Manhattan	2,311,542	2,590,455	794	756	754	1,471	450	58	16.31	15.23	15.18
The Bronx	430,980	705,742	180	146	129	271	59	17	14.63	10.79	9.54
Brooklyn	1,634,351	1,990,614	502	426	459	843	284	36	13.67	11.17	12.03
Queens	284,041	417,107	114	96	91	174	29	5	15.15	12.01	11.38
†Richmond	85,969	102,614	38	30	27	30	13	2	19.99	18.30	13.73
City of New York	4,766,883	5,806,532	1,628	1,460	1,460	2,789	835	118	15.21	13.12	....

*Corrected according to borough of residence.
†The presence of several large institutions, the great majority of whose inmates are non-residents of the city, increases considerably the death-rate of this Borough.

Deaths by Principal Causes, According to Locality and Age.

Boroughs.	Contagious Diseases detailed elsewhere.	Tuberculosis Pulmonalis.	Cerebro-Spinal Meningitis.	Bronchitis.	Diarrhœal Diseases.	Diarrhœal Diseases under 5 Years.	Pneumonia.	Broncho Pneumonia.	Suicides.	Homicides.	Accidents.	Under 1 Year.	Under 5 Years.	5-65 Years.	65 Years and Over.
Manhattan	26	98	1	7	13	12	60	66	8	4	25	154	207	405	144
The Bronx	8	33	..	2	3	3	11	9	2	..	5	22	38	88	20
Brooklyn	17	34	1	8	14	13	42	29	4	1	10	73	101	214	111
Queens	5	15	..	1	1	1	10	4	1	1	2	14	20	56	20
Richmond	..	10	..	..	..	..	4	4	..	..	1	3	6	19	11
Total	56	190	2	18	31	29	127	112	15	6	43	266	372	782	306

Corrected Mortality Among Children.

Boroughs	Under 1 Year of Age. All Causes.	Under 1 Year of Age. Rate per 1,000 Births.	Under 1 Year of Age. Diarrhœal Diseases. Deaths.	Under 1 Year of Age. Diarrhœal Diseases. Rate per 1,000 Births.	Under 1 Year of Age. Diarrhœal Diseases. Institutions.	Under 1 Year of Age. Diarrhœal Diseases. Tenements.	Under 5 Years of Age. All Causes.	Under 5 Years of Age. Rate per 1,000 Living.	Under 5 Years of Age. Diarrhœal Diseases.	Under 5 Years of Age. Rate per 1,000 Living.	Under 5 Years of Age. *Epidemic Diseases.	Under 5 Years of Age. Rate per 1,000 Living.
Manhattan	148	118.0	9	7.2	4	5	201	40.1	12	2.4	20	4.0
The Bronx	23	76.4	1	3.3	..	1	39	26.7	3	2.1	7	4.8
Brooklyn	76	82.2	12	13.0	8	4	104	24.3	13	3.1	10	2.3
Queens	15	87.7	1	5.8	..	1	21	23.4	1	1.1	4	4.5
Richmond	4	88.9	..	....	..	..	7	34.6	..	..	..	....
City of New York	266	98.7	23	8.5	12	11	472	39.8	29	2.5	41	3.5

*Includes Small Pox, Measles, Scarlet Fever, Diphtheria and Whooping Cough.

Infectious and Contagious Diseases in Hospital.

	Willard Parker Hospital. Scarlet Fever.	Diphtheria.	Measles.	Miscel.	Total.	Riverside Hospital. Scarlet Fever.	Diphtheria.	Measles.	Tuberculosis	Miscel.	Total.	Kingston Ave. Hospital. Scarlet Fever.	Diphtheria.	Measles.	Small pox.	Miscel.	Total.	Otisville Sanatorium. Tuberculosis Pulmonalis.
Remaining Jan. 23, 1915	175	102	40	5	322	42	40	5	253	2	342	74	78	32	..	19	203	570
Admitted	34	47	10	1	92	11	13	4	4	..	32	388	31	5	..	8	82	10
Discharged	17	26	12	1	56	3	12	1	5	..	21	7	21	2	..	6	36	12
Died	3	6	1	..	10	..	3	..	1	..	4	2	3	..	..	1	6	..
Remaining Jan. 30, 1915	189	117	37	5	348	50	38	8	251	2	349	103	85	35	..	20	243	568
Total treated	209	149	50	6	414	53	53	9	257	2	374	112	109	37	..	27	285	580

51

Figure 17: Weekly Bulletins Vol 1: Sample Page from 1915.

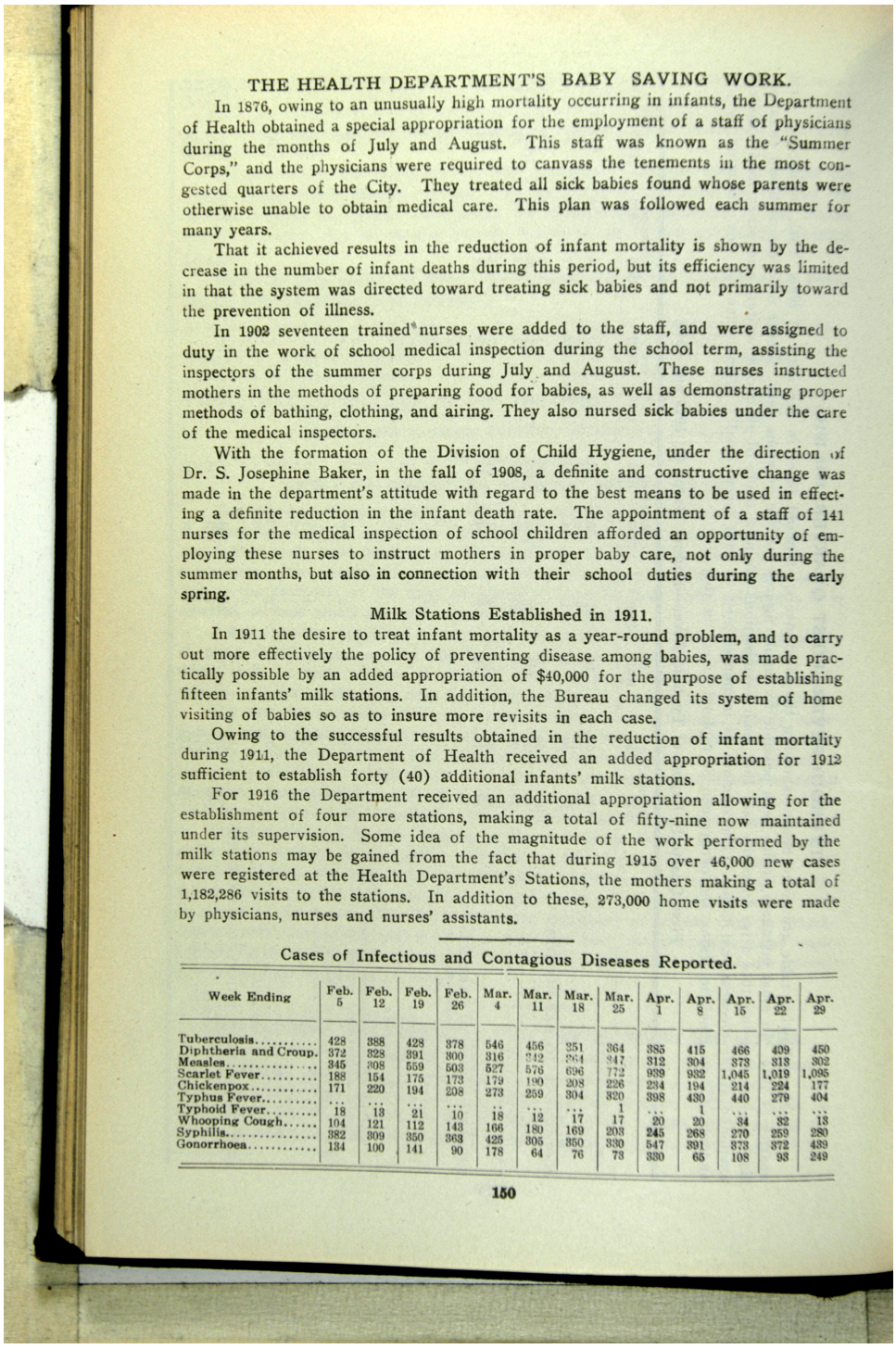

THE HEALTH DEPARTMENT'S BABY SAVING WORK.

In 1876, owing to an unusually high mortality occurring in infants, the Department of Health obtained a special appropriation for the employment of a staff of physicians during the months of July and August. This staff was known as the "Summer Corps," and the physicians were required to canvass the tenements in the most congested quarters of the City. They treated all sick babies found whose parents were otherwise unable to obtain medical care. This plan was followed each summer for many years.

That it achieved results in the reduction of infant mortality is shown by the decrease in the number of infant deaths during this period, but its efficiency was limited in that the system was directed toward treating sick babies and not primarily toward the prevention of illness.

In 1902 seventeen trained nurses were added to the staff, and were assigned to duty in the work of school medical inspection during the school term, assisting the inspectors of the summer corps during July and August. These nurses instructed mothers in the methods of preparing food for babies, as well as demonstrating proper methods of bathing, clothing, and airing. They also nursed sick babies under the care of the medical inspectors.

With the formation of the Division of Child Hygiene, under the direction of Dr. S. Josephine Baker, in the fall of 1908, a definite and constructive change was made in the department's attitude with regard to the best means to be used in effecting a definite reduction in the infant death rate. The appointment of a staff of 141 nurses for the medical inspection of school children afforded an opportunity of employing these nurses to instruct mothers in proper baby care, not only during the summer months, but also in connection with their school duties during the early spring.

Milk Stations Established in 1911.

In 1911 the desire to treat infant mortality as a year-round problem, and to carry out more effectively the policy of preventing disease among babies, was made practically possible by an added appropriation of $40,000 for the purpose of establishing fifteen infants' milk stations. In addition, the Bureau changed its system of home visiting of babies so as to insure more revisits in each case.

Owing to the successful results obtained in the reduction of infant mortality during 1911, the Department of Health received an added appropriation for 1912 sufficient to establish forty (40) additional infants' milk stations.

For 1916 the Department received an additional appropriation allowing for the establishment of four more stations, making a total of fifty-nine now maintained under its supervision. Some idea of the magnitude of the work performed by the milk stations may be gained from the fact that during 1915 over 46,000 new cases were registered at the Health Department's Stations, the mothers making a total of 1,182,286 visits to the stations. In addition to these, 273,000 home visits were made by physicians, nurses and nurses' assistants.

Cases of Infectious and Contagious Diseases Reported.

Week Ending	Feb. 5	Feb. 12	Feb. 19	Feb. 26	Mar. 4	Mar. 11	Mar. 18	Mar. 25	Apr. 1	Apr. 8	Apr. 15	Apr. 22	Apr. 29
Tuberculosis	428	388	428	378	546	456	351	364	385	415	466	409	450
Diphtheria and Croup.	372	328	391	300	316	242	264	347	312	304	373	313	302
Measles	345	308	559	503	527	576	696	772	939	932	1,045	1,019	1,095
Scarlet Fever	188	154	175	173	179	190	208	226	234	194	214	224	177
Chickenpox	171	220	194	208	273	259	304	320	398	430	440	279	404
Typhus Fever	...	...	...	...	..	...	...	1	...	1	...	...	...
Typhoid Fever	18	18	21	10	18	12	17	17	20	20	34	32	18
Whooping Cough	104	121	112	143	166	180	169	203	245	268	270	259	280
Syphilis	382	309	350	363	425	305	350	330	547	391	373	372	439
Gonorrhoea	134	100	141	90	178	64	76	73	330	65	108	93	249

Figure 18: Weekly Bulletins Vol 2: Only Relevant Data Page

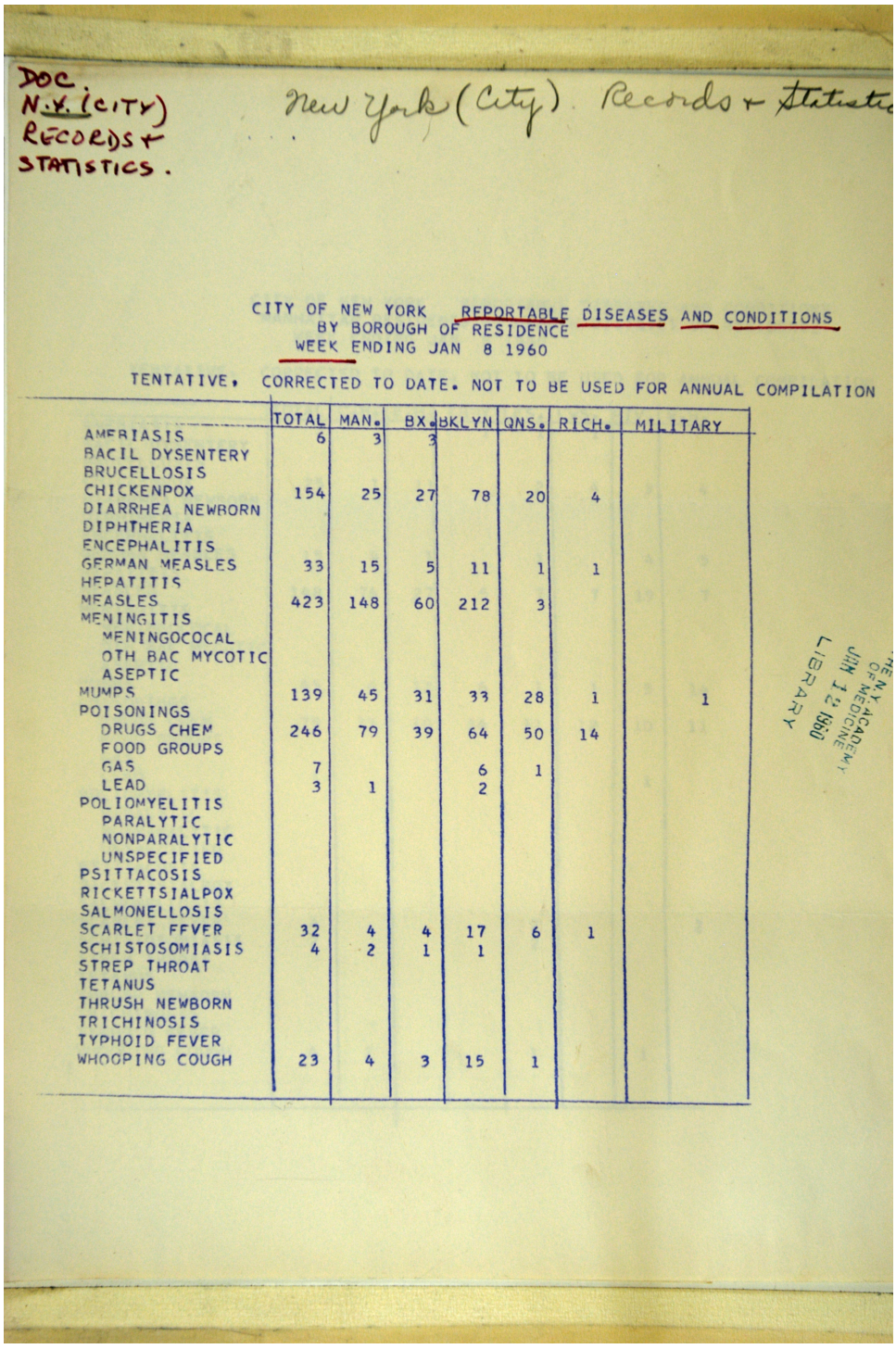

DOC
N.Y. (CITY)
RECORDS +
STATISTICS.

New York (City). Records + Statistic

CITY OF NEW YORK REPORTABLE DISEASES AND CONDITIONS
BY BOROUGH OF RESIDENCE
WEEK ENDING JAN 8 1960

TENTATIVE. CORRECTED TO DATE. NOT TO BE USED FOR ANNUAL COMPILATION

	TOTAL	MAN.	BX.	BKLYN	QNS.	RICH.	MILITARY
AMEBIASIS	6	3	3				
BACIL DYSENTERY							
BRUCELLOSIS							
CHICKENPOX	154	25	27	78	20	4	
DIARRHEA NEWBORN							
DIPHTHERIA							
ENCEPHALITIS							
GERMAN MEASLES	33	15	5	11	1	1	
HEPATITIS							
MEASLES	423	148	60	212	3		
MENINGITIS							
MENINGOCOCAL							
OTH BAC MYCOTIC							
ASEPTIC							
MUMPS	139	45	31	33	28	1	1
POISONINGS							
DRUGS CHEM	246	79	39	64	50	14	
FOOD GROUPS							
GAS	7			6	1		
LEAD	3	1		2			
POLIOMYELITIS							
PARALYTIC							
NONPARALYTIC							
UNSPECIFIED							
PSITTACOSIS							
RICKETTSIALPOX							
SALMONELLOSIS							
SCARLET FEVER	32	4	4	17	6	1	
SCHISTOSOMIASIS	4	2	1	1			
STREP THROAT							
TETANUS							
THRUSH NEWBORN							
TRICHINOSIS							
TYPHOID FEVER							
WHOOPING COUGH	23	4	3	15	1		

Figure 19: Health Department Records: Page 1

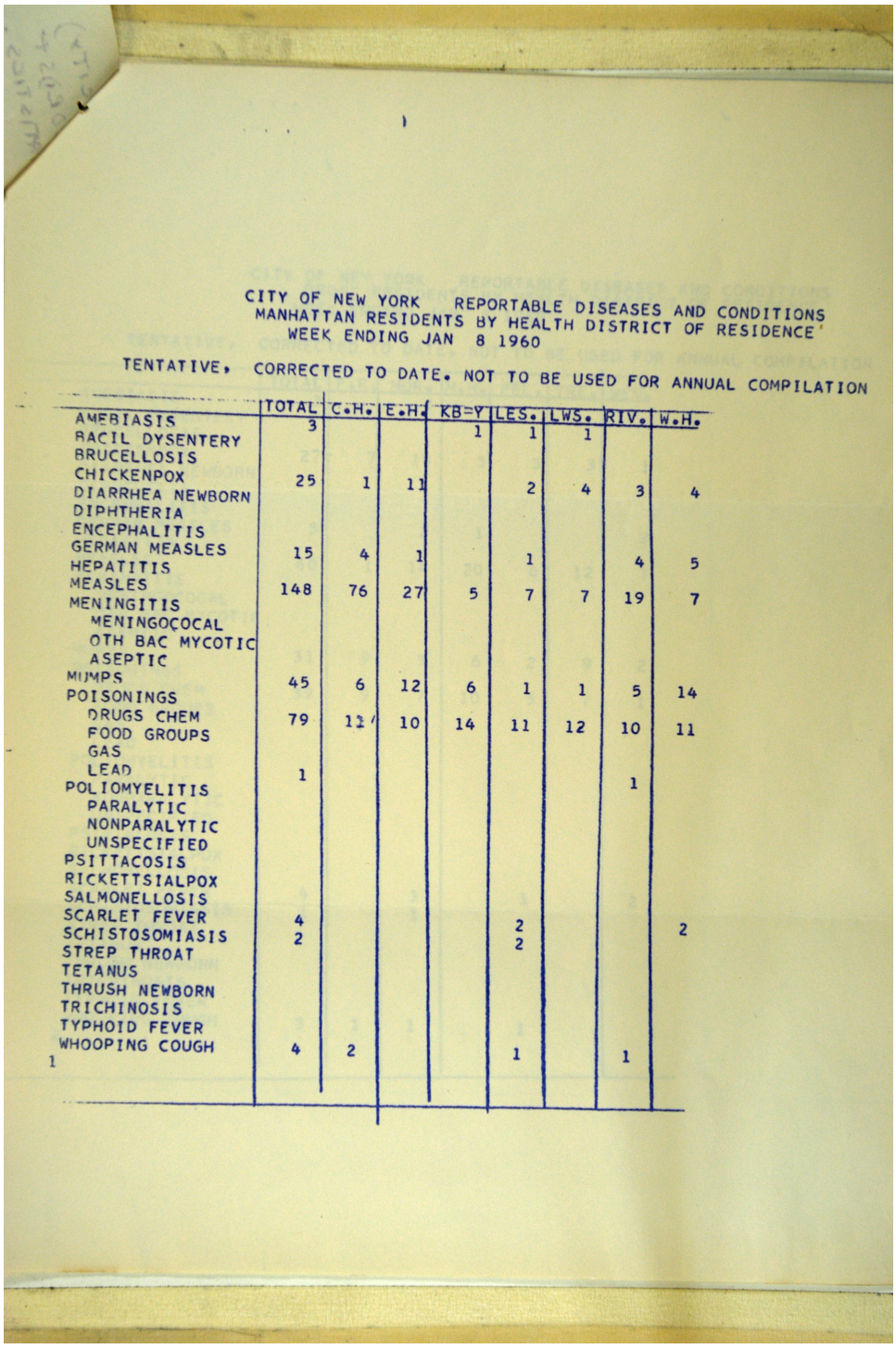

CITY OF NEW YORK REPORTABLE DISEASES AND CONDITIONS
MANHATTAN RESIDENTS BY HEALTH DISTRICT OF RESIDENCE
WEEK ENDING JAN 8 1960

TENTATIVE, CORRECTED TO DATE, NOT TO BE USED FOR ANNUAL COMPILATION

	TOTAL	C.H.	E.H.	KB=Y	LES.	LWS.	RIV.	W.H.
AMEBIASIS	3							
BACIL DYSENTERY				1	1	1		
BRUCELLOSIS								
CHICKENPOX	25	1	11		2	4	3	4
DIARRHEA NEWBORN								
DIPHTHERIA								
ENCEPHALITIS								
GERMAN MEASLES	15	4	1		1		4	5
HEPATITIS								
MEASLES	148	76	27	5	7	7	19	7
MENINGITIS								
MENINGOCOCAL								
OTH BAC MYCOTIC								
ASEPTIC								
MUMPS	45	6	12	6	1	1	5	14
POISONINGS								
DRUGS CHEM	79	11	10	14	11	12	10	11
FOOD GROUPS								
GAS								
LEAD	1						1	
POLIOMYELITIS								
PARALYTIC								
NONPARALYTIC								
UNSPECIFIED								
PSITTACOSIS								
RICKETTSIALPOX								
SALMONELLOSIS								
SCARLET FEVER	4				2			2
SCHISTOSOMIASIS	2				2			
STREP THROAT								
TETANUS								
THRUSH NEWBORN								
TRICHINOSIS								
TYPHOID FEVER								
WHOOPING COUGH	4	2			1		1	

Figure 20: Health Department Records: Page 2

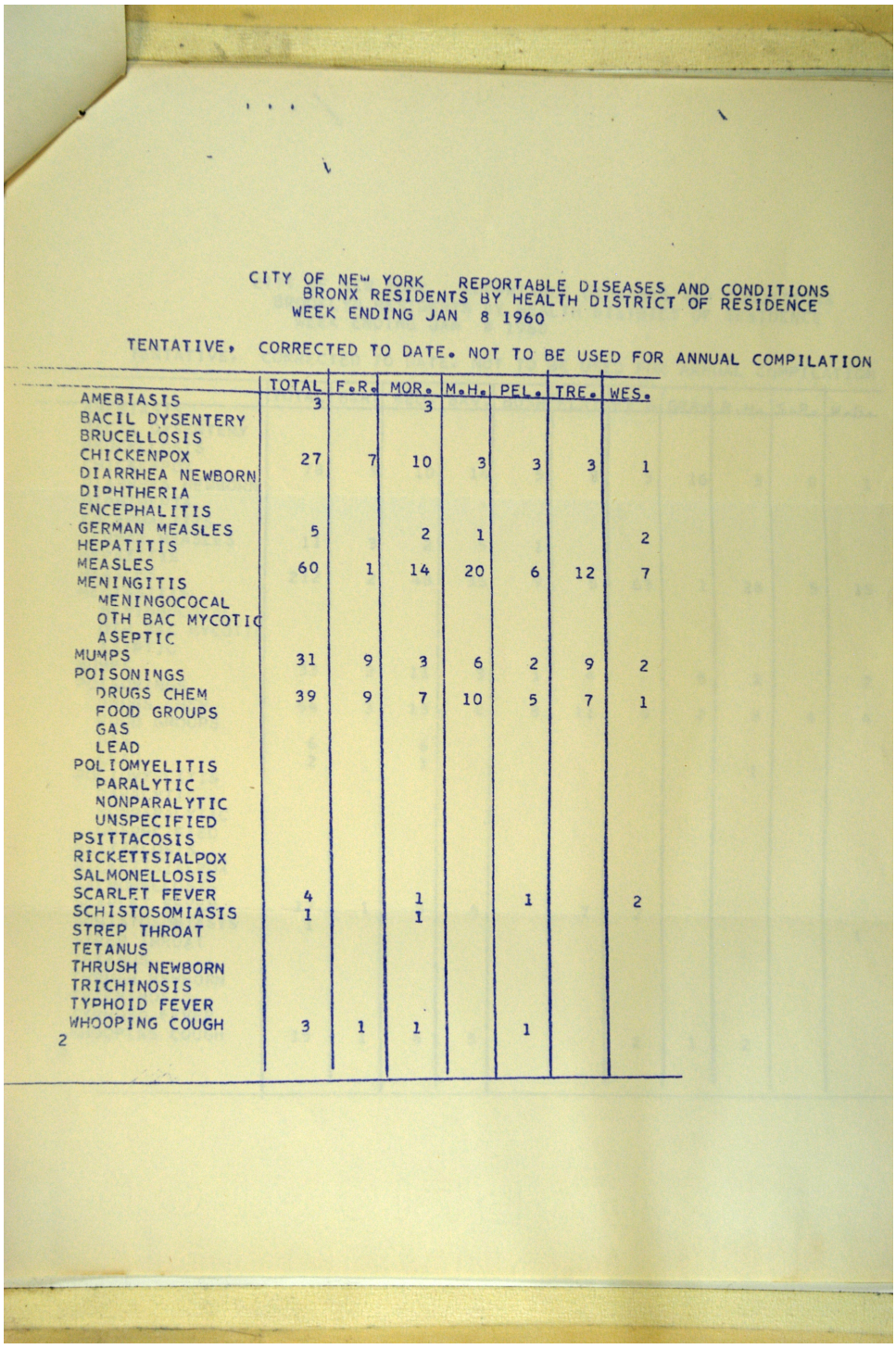

CITY OF NEW YORK REPORTABLE DISEASES AND CONDITIONS
BRONX RESIDENTS BY HEALTH DISTRICT OF RESIDENCE
WEEK ENDING JAN 8 1960

TENTATIVE, CORRECTED TO DATE. NOT TO BE USED FOR ANNUAL COMPILATION

	TOTAL	F.R.	MOR.	M.H.	PEL.	TRE.	WES.
AMEBIASIS	3		3				
BACIL DYSENTERY							
BRUCELLOSIS							
CHICKENPOX	27	7	10	3	3	3	1
DIARRHEA NEWBORN							
DIPHTHERIA							
ENCEPHALITIS							
GERMAN MEASLES	5		2	1			2
HEPATITIS							
MEASLES	60	1	14	20	6	12	7
MENINGITIS							
MENINGOCOCAL							
OTH BAC MYCOTIC							
ASEPTIC							
MUMPS	31	9	3	6	2	9	2
POISONINGS							
DRUGS CHEM	39	9	7	10	5	7	1
FOOD GROUPS							
GAS							
LEAD							
POLIOMYELITIS							
PARALYTIC							
NONPARALYTIC							
UNSPECIFIED							
PSITTACOSIS							
RICKETTSIALPOX							
SALMONELLOSIS							
SCARLET FEVER	4		1		1		2
SCHISTOSOMIASIS	1		1				
STREP THROAT							
TETANUS							
THRUSH NEWBORN							
TRICHINOSIS							
TYPHOID FEVER							
WHOOPING COUGH	3	1	1		1		

2

Figure 21: Health Department Records: Page 3

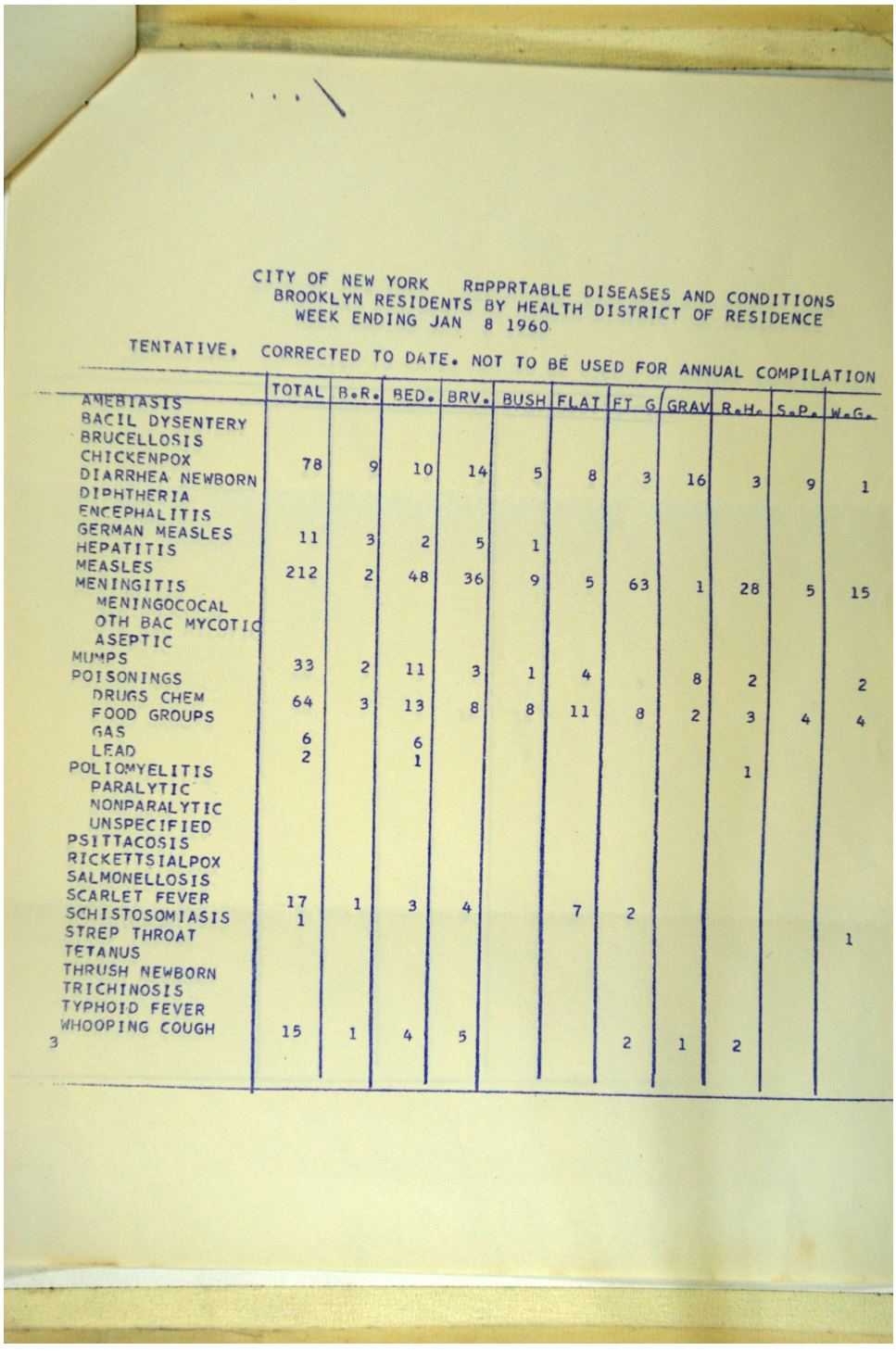

CITY OF NEW YORK REPORTABLE DISEASES AND CONDITIONS
BROOKLYN RESIDENTS BY HEALTH DISTRICT OF RESIDENCE
WEEK ENDING JAN 8 1960

TENTATIVE, CORRECTED TO DATE. NOT TO BE USED FOR ANNUAL COMPILATION

	TOTAL	B.R.	BED.	BRV.	BUSH	FLAT	FT G	GRAV	R.H.	S.P.	W.G.
AMEBIASIS											
BACIL DYSENTERY											
BRUCELLOSIS											
CHICKENPOX	78	9	10	14	5	8	3	16	3	9	1
DIARRHEA NEWBORN											
DIPHTHERIA											
ENCEPHALITIS											
GERMAN MEASLES	11	3	2	5	1						
HEPATITIS											
MEASLES	212	2	48	36	9	5	63	1	28	5	15
MENINGITIS											
MENINGOCOCAL											
OTH BAC MYCOTIC											
ASEPTIC											
MUMPS	33	2	11	3	1	4		8	2		2
POISONINGS											
DRUGS CHEM	64	3	13	8	8	11	8	2	3	4	4
FOOD GROUPS											
GAS	6		6								
LEAD	2		1						1		
POLIOMYELITIS											
PARALYTIC											
NONPARALYTIC											
UNSPECIFIED											
PSITTACOSIS											
RICKETTSIALPOX											
SALMONELLOSIS											
SCARLET FEVER	17	1	3	4		7	2				1
SCHISTOSOMIASIS	1										
STREP THROAT											
TETANUS											
THRUSH NEWBORN											
TRICHINOSIS											
TYPHOID FEVER											
WHOOPING COUGH	15	1	4	5			2	1	2		

3

Figure 22: Health Department Records: Page 4

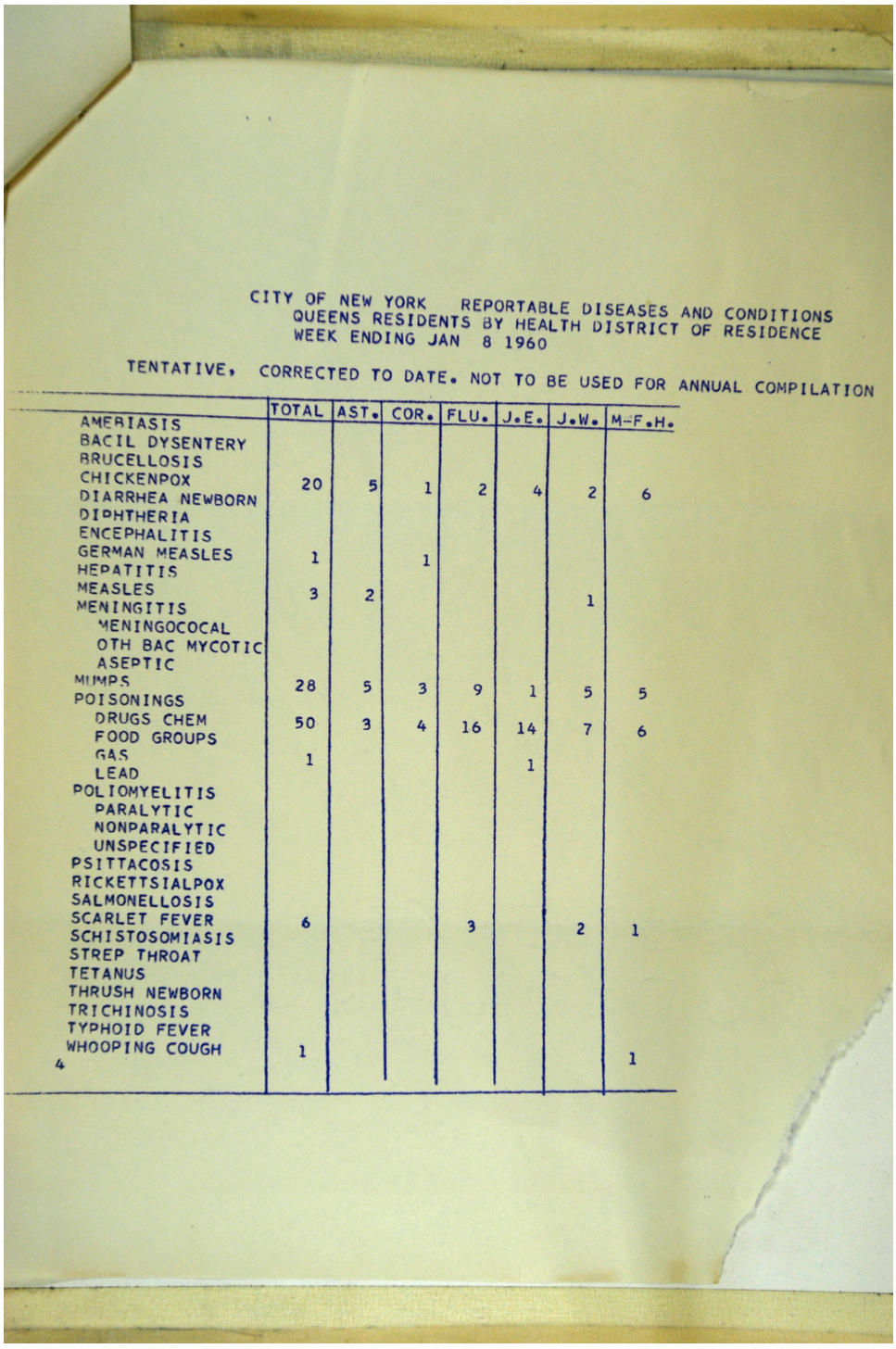

CITY OF NEW YORK REPORTABLE DISEASES AND CONDITIONS
QUEENS RESIDENTS BY HEALTH DISTRICT OF RESIDENCE
WEEK ENDING JAN 8 1960

TENTATIVE, CORRECTED TO DATE. NOT TO BE USED FOR ANNUAL COMPILATION

	TOTAL	AST.	COR.	FLU.	J.E.	J.W.	M-F.H.
AMEBIASIS							
BACIL DYSENTERY							
BRUCELLOSIS							
CHICKENPOX	20	5	1	2	4	2	6
DIARRHEA NEWBORN							
DIPHTHERIA							
ENCEPHALITIS							
GERMAN MEASLES	1		1				
HEPATITIS							
MEASLES	3	2				1	
MENINGITIS							
MENINGOCOCAL							
OTH BAC MYCOTIC							
ASEPTIC							
MUMPS	28	5	3	9	1	5	5
POISONINGS							
DRUGS CHEM	50	3	4	16	14	7	6
FOOD GROUPS							
GAS	1				1		
LEAD							
POLIOMYELITIS							
PARALYTIC							
NONPARALYTIC							
UNSPECIFIED							
PSITTACOSIS							
RICKETTSIALPOX							
SALMONELLOSIS							
SCARLET FEVER	6			3		2	1
SCHISTOSOMIASIS							
STREP THROAT							
TETANUS							
THRUSH NEWBORN							
TRICHINOSIS							
TYPHOID FEVER							
WHOOPING COUGH	1						1

4

Figure 23: Health Department Records: Page 5

References

[1] New York City Department of Health and Mental Hygiene, Office of Vital Records. Summary of Vital Statistcs, 1961-2007 Archived Reports. Available from: http://www.nyc.gov/html/doh/html/vr/vr-archives.shtml.

[2] New York Academy of Medicine. 1216 5th Avenue, New York, NY 10029, United States. www.nyam.org.

[3] M Johansson, Biologist at the CDC. WaveletPackage 2.0, R package. Produces a continuous wavelet transform from an inputted time-series. Received Feb. 2011.

[4] R. M. Anderson and R. M. May. *Infectious Diseases of Humans: Dynamics and Control*. Oxford University Press, Oxford, 1991.

[5] C. T. Bauch and D. J. D. Earn. Interepidemic intervals in forced and unforced seir models. In S. Ruan, G. Wolkowicz, and J. Wu, editors, *Dynamical Systems and Their Applications in Biology*, volume 36 of *Fields Institute Communications*, pages 33–44. American Mathematical Society, Toronto, 2003.

[6] C. T. Bauch and D. J. D. Earn. Transients and attractors in epidemics. *Proceedings of the Royal Society of London, Series* B, 270(1524):1573–1578, 2003.

[7] A. J. Black and A. J. McKane. Stochasticity in staged models of epidemics: quantifying the dynamics of whooping cough. *Journal of the Royal Society Interface*, page doi: 10.1098/rsif.2009.0514, 2010.

[8] B. M. Bolker and B. T. Grenfell. Chaos and biological complexity in measles dynamics. *Proceedings of the Royal Society of London, Series B, Biological Sciences*, 251:75–81, 1993.

[9] B. Cazelles, M. Chavez, G. C. de Magny, J. F. Guegan, and S. Hales. Time-dependent spectral analysis of epidemiological time-series with wavelets. *Journal Of The Royal Society Interface*, 4(15):625–636, 2007.

[10] D. J. D. Earn. Mathematical epidemiology of infectious diseases. In M. A. Lewis, M. A. J. Chaplain, J. P. Keener, and P. K. Maini, editors, *Mathematical Biology*, volume 14 of *IAS/ Park City Mathematics Series*, pages 151–186. American Mathematical Society, 2009.

[11] D. J. D. Earn, P. Rohani, B. M. Bolker, and B. T. Grenfell. A simple model for complex dynamical transitions in epidemics. *Science*, 287(5453):667–670, 2000.

[12] B. Ermentrout. *Simulating, analyzing, and animating dynamical systems: a guide to XPPAUT for researchers and students*. Software, Environments, and Tools. Society for Industrial and Applied Mathematics, Philadelphia, 2002.

[13] D. He and D. J. D. Earn. Epidemiological effects of seasonal oscillations in birth rates. *Theoretical Population Biology*, 72:274–291, 2007.

[14] H. W. Hethcote. The mathematics of infectious diseases. *SIAM Review*, 42(4):599–653, 2000.

[15] G. Hooker, S. P. Ellner, L. De Vargas Roditi, and D. J. D. Earn. Parameterizing state-space models for infectious disease dynamics by generalized profiling: measles in Ontario. *Journal of the Royal Society Interface*, 8(60):961–974, 2011.

[16] M. J. Keeling and B. T. Grenfell. Understanding the persistence of measles: reconciling theory, simulation and observation. *Proceedings of the Royal Society of London Series B-Biological Sciences*, 269(1489):335–343, 2002.

[17] W. O. Kermack and A. G. McKendrick. A contribution to the mathematical theory of epidemics. *Proceedings of the Royal Society of London Series A*, 115:700–721, 1927.

[18] O. Krylova. *Predicting epidemiological transitions in infectious disease dynamics: Smallpox in historic London (1664-1930)*. Phd, McMaster University, Canada, 2011.

[19] O. Krylova and D. J. D. Earn. Effects of the infectious period distribution on predicted transitions in childhood disease dynamics. *preprint*, .

[20] W. London and J. A. Yorke. Recurrent outbreaks of measles, chickenpox and mumps. I. seasonal variation in contact rates. *American Journal of Epidemiology*, 98(6):453–468, 1973.

[21] J. Ma and Z. Ma. Epidemic threshold conditions for seasonally forced SEIR models. *Mathematical Biosciences and Engineering*, 3(1):161–172, 2006.

[22] L. F. Olsen and W. M. Schaffer. Chaos versus noisy periodicity: alternative hypotheses for childhood epidemics. *Science*, 249:499–504, 1990.

[23] D. A. Rand and H. B. Wilson. Chaotic stochasticity: a ubiquitous source of unpredictability in epidemics. *Proc. R. Soc. Lond. B*, 246:179–184, 1991.

[24] C. Torrence and G. P. Compo. A practical guide to wavelet analysis. *Bulletin of American Meteorological Society*, 79(1):61–78. http://atoc.colorado.edu/research/wavelets/, 1998.